Northwest Atlantic Fisheries Organization

Serial No. N6961 **NAFO SCR Doc. 19/040**

SCIENTIFIC COUNCIL MEETING – JUNE 2019

Revisiting Environmental Conditions in the Labrador Sea during 2017

Igor Yashayaev, Marc Ringuette, Ingrid Peterson, Zeliang Wang, Erica Head, Emmanuel Devred

Department of Fisheries and Oceans, Maritimes Region
Ocean and Ecosystem Sciences Division, Bedford Institute of Oceanography
P.O. Box 1006, Dartmouth, N.S. B2Y 4A2

Abstract

In the Labrador Sea, wintertime surface heat losses result in the formation of dense waters which plays an important role in ventilating the deep ocean and driving the global ocean overturning circulation. In the winter of 2016-17, as in the previous winter, the mid-high latitude North Atlantic experienced more moderate surface heat loss in the region than in the winter of 2014-15, characterized by the highest heat losses in more than two decades. In 2016-17, the winter North Atlantic Oscillation index still exceeded its 1981-2010 mean, but its value (2.7 mb) was significantly lower than the 2014-15 value which was the largest in 122 years. However, the surface conditions showed positive air temperature anomaly ranging from 1°C to 4°C over the Labrador Sea, positive sea surface temperature anomalies about 1.5°C, and a slightly lower than normal Labrador Shelf ice extent in the winter. Despite a reduction in the cumulative heat losses from the sea surface after 2014-15, the depth of winter convection continued to increase resulting in the most significant formation, in terms of volume, density and depth, of Labrador Sea Water (LSW) since 1994 reaching below 2000 m. This is mainly due to the water column preconditioning caused by convective mixing in the previous years. Bedford Institute of Oceanography North Atlantic model simulations suggest however that the strength of the Labrador Current (defined as the barotropic transport) had been declining since 1996. The average current was about 4 Sv and 2 Sv weaker in 2017 and 2016, respectively. Phytoplankton bloom onset occurred earlier than usually in the two shelf regions, but while the duration acted on the Greenland Shelf to bring the magnitude to relatively high levels, the situation was reversed on the Labrador Shelf with a relatively lower than average phytoplankton bloom. Extensive cloud covers form end of April to early June of 2017 reduced the percent coverage of the central region with ocean colour data to less than 20% in any of the seven days composite, and most of the good pixels were provided by the northeast corner of the box. Missing and important portion of the bloom initiation phase made it impossible to estimate its magnitude. As a result of the cancellation of the spring research survey, we were unable to update the rate of decline in pH, previously reported as -0.002 y^{-1} over the 1994-2016 period, nor was it possible to assess the state of *Calanus finmarchicus*, the dominant mesozooplankton in the Labrador Sea, following the record lows reported in 2016.

Introduction

Temperature and salinity in the upper layers of the Labrador Sea respond to many factors, including atmospheric forcing, runoff, precipitation, warm and saline inflows from the adjacent North Atlantic basins and colder fresher water arriving from Arctic and glacier melt. Consequently, the variability in the physical, chemical and biological properties of the upper layer of the Labrador Sea is strongly affected by seasonal, interannual and decadal variability in the affecting factors.

A moderately to anomalously cold winter cooling of the upper layer can result in increase in the surface density cause the water column to mix to great depths. By the end of winter, convective mixing (hence the name of the process – winter convection) may penetrate deeper than 1500 m and in extreme cases deeper than 2000 m. Convection is known to ventilate the deeper ocean with atmospheric gases while pumping the nutrients abundant in the deeper layers back to the surface. Reduced surface heat losses in milder winters lead to weaker convection, and as a result to stronger influence of heat and salt passed from the warm and saline Atlantic Waters. As a result a stronger stratification gets established in the subsurface (>200 m) and deeper layers during the period of convective relaxation. Year-specific atmospheric conditions, partly expressed in cumulative heat flux and climate indices play a dominant role in setting the deep convection events in the Labrador Sea, which can help explain development of significant long-term oceanographic phenomena in the region. One of such climate indices is the North Atlantic Oscillation (NAO) index expressing the strength of zonal atmospheric circulation in the North Atlantic. An increase in zonal wind is often associated with strengthening of the atmospheric forcing and higher heat losses in winter. Under the global warming scenarios, the increasing freshwater inputs from Greenland glacier melting and the Arctic also contribute to the oceanographic variations at seasonal, inter-annual and longer time scales. However, the recent study suggests (DD, 2019) that the effect of Greenland freshwater flux anomaly associated with lacier melting is not sufficient at the moment to explain the present changes in water column salinity and convective activity. However, the future may bring a different example, especially if melt continues to accelerate.

While there has been relatively little variability below 2500 m, there have been significant decade-long events in the upper 2000 m. A period of warming and increasing salinity during the mid-1960s to mid-1970s was followed by an inverse period of cooling and freshening during the 1990s. This period was characterized by deep winter convection that filled the upper 2.0 to 2.5 kilometers of the Labrador Sea with cold, dense and relatively fresh water. Milder winters in the early 2000s produced more limited amounts of mode waters, which have gradually become warmer, saltier, and less dense than in the previous decade. The cessation of extreme convection in the mid-1990s led to the upward temperature and downward density trends spanning the upper 1000 m of the water column that were interrupted in the winters of 1999-2000, 2001-02, 2007-08 and 2011-12, and finally reversed in 2013-14, when deep convection was observed reaching and exceeding the depth of 1500 m over significant parts of the central Labrador Sea. In the four most recent consecutive winters, 2013-14, 2014-15, 2015-16 and 2016-17, deep convection kept getting deeper and deeper with each new event, while the convectively formed water mass, so-called Labrador Sea Water (LSW), was getting colder and denser as convection deepened. The environmental conditions that contributed to the case of deep convection in 2007-08 have been documented by Yashayaev and Loder (2009). The most recent intensification of winter convection, 2011-12 through 2015-16, has been analyzed by Yashayaev and Loder (2016 and 2017). Finally, the most recent episode of deepening convection, 2016-17, is presented in this report.

About one quarter of carbon dioxide (CO_2) released by human activities (anthropogenic CO_2, mainly due to fossil fuel combustion) has been taken up by the oceans, altering the basic ocean chemistry, specifically the marine carbonate system. The Labrador Sea is the site of a strong "solubility pump"; anthropogenic CO_2 sequestrated from the atmosphere is transported to the deep ocean by chemical and physical processes. On the flip side however, the dissolution of anthropogenic CO_2 also has decreased ocean pH by 0.1 units over the past 200 years, corresponding to a 30% increase in acidity (Caldeira and Wickett, 2003). If global emissions of CO_2 continue at their present rate, ocean pH is predicted to fall an additional 0.3 units by 2100. The oceans have not experienced such a rapid pH decrease (ocean acidification) or one of this great a magnitude for at least 20 million years (Feely et al., 2004), raising serious concerns about the ability of marine ecosystems to adapt. The major impact of decreasing pH will be felt by organisms that form calcium carbonate ($CaCO_3$) shells and skeletons,

because rising acidity increases the solubility of $CaCO_3$. Since $CaCO_3$ shells and skeletons are naturally more soluble at lower temperatures and higher pressures, high latitude and deep water ecosystems will be more vulnerable to the added stress of ocean acidification. Furthermore, rapid environmental changes such as retreating ice extent and enhanced hydrological cycles may amplify these problems.

Light limits primary production and phytoplankton communities succession for much of the year (Harrison and Li, 2008; Fragoso et al, 2016) and Shallow mixed layer and Nitrate is limiting growth on the Labrador Shelf while Silicate seems to be the limiting factor for growth in the Labrador Basin (Harrison and Li 2008). These conditions favour the emergence of *Phaeocystis pouchetii* in the North and Eastern part of the Labrador Sea (Fragoso et al 2016). The Labrador Shelf, mostly under the influence of Arctic water masses, is dominated by polar diatom species (*Thalassiosira* spp. and *Bacteriosira bathyomphala*) and species associated with costal melting ice (*Porosira glacialis* and *Fossula arctica)*. Primary production patterns, such mesoscale features leave their imprint in mesozooplankton distribution and abundances (Yebra et al 2009). One species of copepod, *Calanus finmarchicus*, dominates the mesozooplankton biomass throughout the central region of the Labrador Sea, while on the shelves two Arctic *Calanus* species, *C. glacialis* and *C. hyperboreus*, are equally important. *C. finmarchicus* abundances show regional variations that are generally consistent from year-to-year and are related to differences in the timing of the life-cycle events, which are themselves influenced by environmental conditions. In spring, populations here generally have few young stages from the new years' generations, and these, and total abundances, increase in summer. Total abundance in spring showed an upward but insignificant trend on the Labrador Shelf between 1996 and 2012. In the Central Labrador Sea total *C. finmarchicus* abundance is generally relatively low in spring and summer, with a low proportion of young stages; one exception being the summer of 1995, when young stages were dominant and total abundance was relatively high. There was no trend in springtime total abundance between 1996 and 2012 and the abundance in 2012 was within the range seen in previous springs. *C. finmarchicus* abundances are generally higher in the eastern Labrador Sea (the area most influenced by the Irminger Current) than farther west in spring, because the spring bloom starts earlier here, which leads to earlier reproduction in *C. finmarchicus*. Although abundances are generally higher here in summer than in spring, the highest concentration of all occurred in spring 2006. The abundance in 2012 was within the range of values seen in previous springs and there was no trend in springtime abundance between 1996 and 2012.

Production variability in the lower trophic compartments eventually impacts the higher trophic growth and recruitment and ultimately influences commercial fisheries in the region.

Since 1990, the Ocean and Ecosystem Sciences Division at the Bedford Institute of Oceanography has carried out annual occupations of an oceanographic section across the Labrador Sea (Figure 1). The section was designated as AR7W (Atlantic Repeat Hydrography Line 7 West) in the World Ocean Circulation Experiment (WOCE) hydrography line classification (notation). These surveys cover a wide range of physical and chemical characteristics and properties of seawater, e.g., temperature, salinity, density, currents, dissolved oxygen, nutrients, chlorofluorocarbons, sulfur hexafluoride, total inorganic carbon, pH, oxygen and iodine isotopes, and measurements of important biological and ecosystem variables, e.g., bacteria until 2012, phytoplankton and mesozooplankton.

The AR7W oceanographic line is presently regarded as the major component of the Atlantic Zone Off-shelf Monitoring Program (AZOMP) of Fisheries and Oceans Canada (DFO) and its annual occupation is recognized as the most vital and significant Canadian contribution to the international Global Climate Observing System (GCOS) and to the (international) Climate Variability (CLIVAR) component of the World Climate Research Programme (WCRP). It is also reported on annually as a part of the environmental synopsis submitted by DFO to the Northwest Atlantic Fisheries organisation (NAFO) for the fish stock assessment within the region. The AR7W section spans approximately 900 km from Misery Point, Labrador, to Cape Desolation, Greenland, however the shelf areas can be out of reach and hence limited in data coverage due to sea-ice condition. With nearly three decades of annual surveys, the time series now allows a examination of multiyear trends in all key ecosystem variables. DFO also contributes to the international Argo program by deploying floats in the Labrador Sea and managing, processing and analysing the Argo data. The annual AZOMP multidisciplinary survey of the Labrador Sea, primarily consisting of AR7W occupations, mooring redeployments and Argo float deployments,

represent an invaluable contribution to the ongoing international ocean and climate monitoring and research effort and is highlight in a recent special issue of Progress in Oceanography (Yashayaev et al., 2015; Kieke and Yashayaev, 2015) and the latest publications in Nature (Thornalley et al., 2018) and Science (Lozier et al., 2019).

In addition to the AR7W Line, a full AZOMP survey also includes sampling of the extended Halifax Line (XHL) to monitor variability on the Scotian Rise and Slope in the deep western boundary flows of the North Atlantic and to obtain additional information on oceanographic properties and lower-trophic-level variability of the Slope Water affecting the Scotian and adjacent shelves (http://www.bio.gc.ca/science/monitoring-monitorage/azomp-pmzao/azomp-pmzao-en.php). In 2017 however, the CCGS *Hudson* was not available due to life extending refits and longer time than expect spent into dry-dock. Several tentative to secure charter vessels at the last minute also failed. Henceforth this year reports relies solely on profiling float data, remote-sensed measurements, reanalysis fields and modelled data.

Data Sources and Methods of Analysis

The state of the Labrador Sea environment in 2017 as presented in this report is based on a mix of profiling float and remote-sensed measurement and reanalysis products. The sources of these data are described in the present section. As noted earlier an AZOMP cruise did not happen in 2017, so there is no associated AR7W data reported for that reason.

Atmospheric Reanalysis

The NCEP/NCAR Reanalysis Project is a joint project between the National Centers for Environmental Prediction (NCEP) and the National Center for Atmospheric Research (NCAR), often referred to as the NCAR/NCEP reanalysis. The goal of this joint effort is to produce new Surface Air Temperature and Sea Surface analysis using historical data (1948 onwards) to produce analyses of the current atmospheric state (Kalnay et al., 1996).

North Atlantic Oscillation Index

The North Atlantic Oscillation (NAO) index used here is the difference in winter (December, January and February) sea level atmospheric pressures between the Azores and Iceland, and is a measure of the strength of the winter westerly winds over the Northwest Atlantic and represents the dominant, large scale meteorological forcing over the North Atlantic Ocean. Specifically, the index was calculated using observed monthly sea level pressures at Ponta Delgada (up to 1997, 2009-2015), Santa Maria (1998-2005), and Lajes (2006-2008) in the Azores, and at Akureyri in Iceland. A small number of missing data early in the time series were filled using pressures from nearby stations.

Ice cover

The sea ice data are obtained from The U.S. National Snow and Ice Data Center.

Profiling Argo Float Data

Argo is an international network of profiling floats collecting high-quality temperature and salinity profiles from the upper 2000 m of the ice-free global ocean and through float displacements currents from intermediate depths. For most of a typical 10-day cycle a battery-powered autonomous float freely drifts at a “parking depth” of usually 1000 m, where its position is stabilised through buoyant adjustment. Once the float is released from its parking depth it descents to approximately 2000 m and then ascents to the surface, while profiling temperature, salinity and other variables, if additional sensors are installed. When the surface is reached the acquired data get transmitted, and the float sinks back to its parking depth. Since 2002, the near real-time temperature and salinity Argo float data collectively draw a large-scale picture of the oceanographic structure and circulation of the Labrador Sea. The array is typically used to reconstruct the seasonal and interannual variability of the physical characteristics and dissolved oxygen in the upper 2000 m water column. The value of the Argo floats

is signified in winter, when they work out to be the only mean to provide information about real-time development of winter convection.

Ocean Colour

Ocean colour, as an indicator of sea surface chlorophyll-*a* concentration (SSC), is derived from the observations made by the Moderate Resolution Imaging Spectroradiometer (MODIS) aboard the Aqua Earth Observing System satellite between 2003 and 2012 and by the Visible Infrared Imaging Radiometer Suite (VIIRS) since 2013. Remotely-sensed images of ocean colour for the Labrador Sea are composited on a 2-week basis from the beginning of March to the end of October each year. Between November and February, the data are usually too sparse to be useful. From these composites, ocean colour data are extracted from 511 pixels comprising the AR7W transect. A biweekly climatology of SSC constructed from the time series of ocean colour from 2003 to 2017 (Figure 13), and fitted with a Gaussian function to extract the principals blooms metrics following Zhai et al (2011). If a satellite composite has less than 20% in spatial data coverage it becomes impossible to compute meaningful blooms indices, particularly in May and June.

Continuous Plankton Recorder Data

The Continuous Plankton Recorder (CPR) is an instrument that is towed by commercial ships that collects plankton at a depth of ~7 m on a long continuous ribbon of silk (~260 μm mesh). The position on the silk corresponds to the location of the different sampling stations. CPR data are analysed to detect changes in indices of phytoplankton concentration (colour and relative numerical abundance) and zooplankton relative abundance for different months, years and/or decades in the northwest Atlantic. The indices indicate relative changes in concentration (Richardson et al. 2006). The sampling methods from the first surveys in the northwest Atlantic (1957 for the sub-polar gyre, 1960 for the Canadian continental shelf) to the present are exactly the same so that valid comparisons can be made between months, years and decades. CPR data collected from January to December 2014 were only made available in January 2016 to add to the DFO data archive.

The tow routes between Reykjavik and the Gulf of Maine are divided into eight regions: the Western Scotian Shelf (WSS), the Eastern Scotian Shelf (ESS), the South Newfoundland Shelf (SNS), the Newfoundland Shelf (NS) and four regions in the NW Atlantic sub-polar gyre, divided into 5 degree of longitude bins (Figure 15). In this report a broad-scale comparison is presented for CPR data collected in all regions and all sampling decades. More detailed analyses for the Scotian Shelf and Newfoundland Shelf regions are presented in the annual AZMP Reports from the Maritimes and Newfoundland Regions. These latter reports concentrate on data collected since 1992, since these are comparable to AZMP survey results, which date back to 1999.

Monthly average abundances ($\log_{10}(N+1)$ transformed for all but PCI) were calculated for 15 CPR taxa by averaging values for all individual samples collected within each region for each month and year. These regional monthly average abundances were then averaged by month for samples collected within each decade prior to 2009, (i.e. 1960-1969, 1970-1979, 1980-1989, 1990-1999 and 2000-2009) to give decadal monthly average abundances, which were then averaged for each decade to give decadal annual average abundances. During the 1980s sampling was too infrequent to calculate decadal annual average abundances, except for the three regions between 30 and 45oW, and even in these regions there was no sampling in January or December. The averages of the monthly values for the 1970s and 1990s were used to fill in these missing months, however, so that decadal annual average abundances could be calculated. The averages of the decadal annual average abundances over the 4 or 5 sampling decades represent the climatological average annual abundances. Four-year annual average abundances were calculated for 2010-2013, using the 4-year monthly averages, and annual average abundances were calculated for 2014, where possible. According to the protocol used here, annual averages for individual years can only be calculated if there was sampling in more than 8 months, with no gaps of more than 2 consecutive months (linear interpolation being used to fill in for missing months). These criteria were met in 7 regions in 2014, for which there were 0-3 missing months, with no 2 or 3 month gaps. No annual average abundances could be calculated for the SNS region in 2014, since there was sampling in only 6 months and a 5 month gap.

Standardized abundance anomalies were calculated for the decadal (1960s, 1970s, 1980s, 1990s, 2000s), four-year (2010-2013) and annual (2014) average abundances, by subtracting the climatological average annual abundances for each time period, and by dividing the differences by the standard deviations calculated for the annual average abundances available for the individual years between 1992 and 2009. Sampling coverage was good everywhere over this period, so that annual averages could be calculated for 13-15 individual years in all regions. The underlying assumption of this approach to the calculation of the standardized abundance anomalies is that inter-annual variability was similar for all decades. This assumption was found to be reasonable for the 1960-1970s in the four regions of the sub-polar gyre, decades for which annual average abundances and standard deviations could be calculated for 15 individual years. As well, it was not inconsistent with results for the shelf regions, where annual averages over the same decades could be calculated for only 2-6 years.

Results and Discussion

Atmospheric Indices and Forcing

The NAO is an important teleconnection pattern influencing atmospheric processes in the Labrador Sea (Barnston and Livezey, 1987; Hausser et al., 2015). The NAO index is based on the surface sea-level pressure difference between the Subtropical (Azores) High and the Subpolar (Icelandic) Low. The positive phase of the NAO reflects below-normal heights and pressure across the high latitudes of the North Atlantic and above-normal heights and pressure over the central North Atlantic, the eastern United States and western Europe. The negative phase reflects an opposite pattern of height and pressure anomalies over these regions. Both NAO phases are associated with basin-wide changes in the intensity and location of the North Atlantic jet stream and storm track, and in large-scale modulations of the zonal and meridional heat and moisture transport (Hurrell, 1995), resulting in the modification of the temperature and precipitation patterns.

The NAO exhibits considerable interseasonal to interdecadal variability, and prolonged periods of both positive and negative phases seem to have more influence on convection in the Labrador Sea than short-term fluctuations (Yashayaev, 2007). Yashayaev and Loder (2017) further showed that the ocean's memory or inter-annual preconditioning plays and important role in switching between the regimes of deeper and shallower convection. Even though this was demonstrated on the cumulative winter heat losses (updated below), a similar connection exists between lag-filtered NAO, convection depth and ocean heat content. The wintertime NAO also exhibits significant multi-decadal variability (Hurrell, 1995). An upward trend of the NAO index from the 1960s through the 1990s was noted by Visbeck et al (2001), although since the peak in the 1990s there has been a slight downward trend. Recent studies reveal an atmospheric circulation pattern, complementary to NAO, which becomes more prominent in years of low NAO (Hausser et al., 2015). Further study of this phenomenon will help to improve understanding and forecasting capabilities of atmospheric and oceanic conditions.

In 2010, the NAO index reached a record low (Figure 2), with surface heat losses being quite low as well, leading to warmer than normal oceanic conditions as we show in both the Argo float and AR7W survey based records. In 2011, the NAO index rebounded from the record low but still remained well below the 30-year average (1981-2010). In 2012, however, the NAO index was strongly positive (12 mbar), up to a level comparable to those in early 1990s showing the highest winter index over the last twenty years. There was a significant change in the winter NAO index in 2013, when it became moderately negative (-3 mbar). In 2014, the NAO index returned to its high positive phase, slightly lower than the 2012 value, making it the second highest in the last twenty years, leading to colder than normal winter conditions in the region. In 2015 there was another high NAO event (17.8 mbar), as a matter of fact, it was the highest value on record. In 2017, the winter NAO index was slightly positive, +2.7 mb (+0.3SD) above the 1981-2010 mean, but significantly smaller than 2015 which was the largest positive value in the 122 year record (Figure 2, upper panel). The lower panels of Figure 2 show the sea level pressure conditions during the winter of 2017 compared to the 1981-2010 mean. The Icelandic low was slightly lower than the long-term average whereas the Azores high was normal. The centers were almost directly over the NAO index sites. As one might expect, there is a high correlation between the reported changes in the NAO index and changes in the surface heat flux integrated for

each cooling season (Figure 3). The cumulative winter heat losses are in turn correlated with the convection depth and heat content.

The NCEP reanalysis of surface air temperature indicates above normal conditions with an anomaly ranging between 1 and 4°C over the Labrador Sea in the winter, and the biggest winter positive anomalies were over the central Labrador Sea of >4°C (Figure 4). Most of the Labrador Sea was at or a little bit below normal during the spring, while the Baffin Bay area had a positive anomaly of ~2°C. In summer, the Labrador Sea and Baffin Bay were similar to those in the spring, with smaller positive anomalies in the Baffin Bay. Fall experienced higher than normal temperature in both Baffin Bay and Labrador Sea, with a higher than 3°C anomaly in the Baffin Bay and 2 to 3°C above normal anomalies in the Labrador Sea (Figure 4).

Sea Surface Temperature

In the Baffin Bay, the warming events for the 4 seasons were present with higher than 1.5°C positive SST anomalies for the most of Baffin Bay. The winter and fall seasons even had anomalies exceeding 2°C for all or most of the whole Baffin Bay (Figure 5).

In the Labrador Sea, during winter, the northern region had positive anomalies ~2°C above the norm, and the southern region had anomalies on the order of ~1.5°C. In spring, slightly colder than normal conditions (~1°C below normal) were found on the Labrador Shelf and in the western part of the sea. However, the eastern portion of the Labrador Sea had a 0.5°C anomaly, and later, during summer, a positive SST anomaly expanded almost across the entire Labrador Sea. In fall, 2°C positive anomalies were present in the western part of the Labrador Sea, while weaker positive anomalies (~1.5°C) were observed along the eastern margin.

Although in agreement with the seasonally averaged NCEP data, the yearly SST average estimated using remote sense AVHRR (NOAA) proves to be colder than average in the three regions we are monitoring at respectively -0.52°C on the Labrador Shelf, at -0.44°C in the Labrador Basin and almost on average for the Greenland Shelf (Figure 14).

Sea Ice Conditions

Ice concentration in the coastal zone of Labrador Shelf was slightly above normal in the winter months of 2017 (5-10%; reference period: 1981-2010), which is similar to the previous year (2016) conditions. The ice extents in the winter months were mostly aligned with the 1981-2010 climatology, though shrinking ice extents were more noticeable in late winter months (Figure 6).

In order to provide a quantitative and clearer view of the ice extent changes in the Davis Strait (63-68°N), the northern Labrador Sea (58-63°N), and the Labrador Shelf (53-58°N), the ice extents for the three regions were estimated by summing the areas with ice concentration higher than 85%. Figure 7 shows the time series of monthly ice extent anomalies from 1979 to 2017, with the monthly mean climatology based on the data from 1981 to 2010. The wintertime ice extent in Davis Strait was slightly below normal (12,000 km^2 below normal), and the northern Labrador Sea ice extent was below normal in wintertime as well as a whole (23,000 km^2 below normal). On the Labrador Shelf, the ice extent was below normal (6,500 Km^2 below normal).

Winter Convection and Hydrographic Conditions in the Central Labrador Sea

The advent of the International Argo Program has provided the oceanographic community with unprecedented, year-round observations of temperature and salinity in the Labrador Sea. In the absence of an oceanographic survey of the AR7W line in spring of 2017, the Argo dataset is our only source of *in-situ* data available for this year. Time-depth distributions of seawater temperature and salinity based on all Argo and ship survey profile data available in the central Labrador Sea for the time period of 2002-2018 in the depth range of 0-2000 m are presented in Figure 8. The time series clearly demonstrates the seasonal and inter-annual variability over the last decade and a half in this region. The deep convection event of 2008 is evident in both the temperature and salinity fields. The conditions in the winter of 2011 were similar to those in the preceding winter with very limited convection (mixed layer depths did not exceed 800 m). Then, in the winter of 2012, convection reached

the depths of ~1400 m, which is clearly present in temperature and salinity profiles acquired by both Argo floats and ship survey. Salinity in the top 200 m in 2012 was the lowest since 2003, particularly in the top 50 m. Convection also occurred in the winter of 2013, but it was not as deep as in the previous year, and was mostly limited to the top 1000 m. The situation changed quite significantly in 2014. Wintertime cooling triggered convective mixing homogenizing the top 1600 m and probably even deeper layer in the central Labrador Sea. Over the following three winters convection developed to nearly 2000 m making this whole part of the water column colder and denser with each cooling cycle. This pattern agrees with previously stated impact of a multiyear recurrence of relatively strong cooling coming in phase with high NAO and resulting in preconditioning of water column which in turn facilitates development of an even deeper convection in a following year even if the strength of winter cooling has declined.

The annual mean water column properties (temperature, salinity and density) averaged over the top 2000 m, NAO index, and cumulated surface heat losses and heat content changes in winter are presented in Figure 9. The effect of water column preconditioning by winter convection of previous years is well reflected in the one-side low-pass filtered curves indicated in the figure.

Other than being the main factor of interannual variability of the intermediate layer throughout the North Atlantic, wintertime convection in the Labrador Sea is a key process driving or strongly influencing the Atlantic Meridional Overturning Circulation (AMOC), and the Labrador Sea steps here as one of the few areas in the global ocean where the surface waters are exchanged with those from much greater depths. This process also has an important role in biogeochemical cycling in the Labrador Sea, and strong convection enhances the entrainment of gases such as oxygen and carbon dioxide into the deep water from the atmosphere, as well as from upper-layer freshwater.

The Labrador Current

The strength and position of the Labrador Current (LC) are important indicators of the state of the subpolar North Atlantic, and closely reflect, precede or follow changes in its circulation, and mass, heat and volume balance. Through winter convection in the Labrador Sea, this region plays an important role in the global climate and state of regional ecosystem. Hence the variations in the LC can to some degree be connected to the variations in the AMOC. Here we present the variations in the LC barotropic transport from an eddy resolving model developed at the Bedford Institute of Oceanography. The model is a 1/12 degree resolution North Atlantic Model (hence the Bedford Institute of Oceanography North Atlantic Model or BNAM) described in detail by Brickman et al. (2015) and Wang et al. (2016).

An EOF analysis of the BNAM output performed by Wang et al. (2016) (reproduced in Figure 10) suggests that the variability in the Labrador Current, and therefore the flow by itself, can be partitioned into two components – the western and eastern Labrador Currents (WLC and ELC), confined to the 300-2500 and 2500-3300 m water depth ranges, respectively. Following these definition we calculated the transports of ELC and WLC, as well as the total LC transport obtained as a sum of the two. The transport calculations used the modelled flows through the western segment of a simulated transect analogous to AR7W.

Figure 11 shows the transport anomalies for the LC, ELC and WLC. It demonstrates that the WLC was still stronger in 2017 than the 1990-2017 mean (by 2.2 Sv), as it had been since 2001. On the other hand, the declining trend in the ELC was continuing since 1996 which was the year with a significant drop in the winter NAO index. Wang et al. (2016) suggested the ELC is an indicator for the changes in the AMOC, which suggests that the declining trend of AMOC was continuing from this model simulation. Just in 2017 the ELC was a little bit more than 6.5 Sv weaker than the mean.

Ocean Color

High cloud coverage during April-June led to a very poor data coverage of the Labrador Sea in 2017, particularly the central part of the region (Figure 12). Over a period of five weeks running form end of April to early June of 2017, the percent coverage in the central region never exceeded 20% in any seven-day composite, and most of the good pixels were provided by the northeast corner of the box. However some conclusions, particularly in the boundary regions could still be made. In both inshore

regions a bloom onset happened earlier than normal in 2017, but while the bloom did persist in its duration on the Greenland Shelf helping to bring the magnitude to relatively high values, the situation was reversed on the Labrador Shelf resulting in a relatively lower than the average phytoplankton bloom.

Generally, the annual phytoplankton spring bloom starts earlier on the Greenland Shelf and Slope (mid-April to May), than in the central Labrador Basin and Labrador Shelf regions (early May to late June). An important exception was the spring of 2015, when the timing of the bloom was shifted to particularly early dates in the central basin, starting mid-April, one of the earliest onset since 2002. While brief, at only about 49 days in duration, this bloom was unusually intense with the highest amplitude ever recorded for the region (over 5 mg m^{-3}) and giving a seasonally integrated value among the highest ever seen. Greenland shelf characteristics followed the same pattern, while the Labrador Shelf bloom metrics were about average for the region. Within the two-dimensional spatial regional boxes defined by Harrison and Li (2008), the SSCs averaged over the period from March to October 2015 were 0.62 mg m^{-3} on the Labrador Shelf, 3.20 mg m^{-3} in the central Labrador Basin, and 1.61 mg m^{-3} on the Greenland Shelf (Figure 13).

Despite continuing convection and general water column cooling the spring bloom observed in 2016 was not as massive as in 2015. The limited data for April and May of 2017 do not allow us to make a broader spatial assessment of the bloom extent; however the few available pixels suggest that the situation with the spring bloom was closer to 2016 than 2015.

Continuous Plankton Recorder (featured section)

The Continuous Plankton Recorder (CPR) is an instrument that is towed by commercial ships that collects plankton at a depth of ~7 m on a long continuous ribbon of silk (~260 µm mesh). The position on the silk corresponds to the location of the different sampling stations. CPR data are analysed to detect changes in indices of phytoplankton concentration (colour and relative numerical abundance) and zooplankton relative abundance for different months, years and/or decades in the northwest Atlantic. The indices indicate relative changes in concentration (Richardson et al. 2006). The sampling methods from the first surveys in the northwest Atlantic (1957 for the sub-polar gyre, 1960 for the Canadian continental shelf) to the present are exactly the same so that valid comparisons can be made between months, years and decades. CPR data collected from January to December 2014 were made available in January 2016 to add to the DFO data archive.

The tow routes between Reykjavik and the Gulf of Maine are divided into eight regions: the Western Scotian Shelf (WSS), the Eastern Scotian Shelf (ESS), the South Newfoundland Shelf (SNS), the Newfoundland Shelf (NS) and four regions in the NW Atlantic sub-polar gyre, divided into 5 degree of longitude bins (Figure 15). In this report a broad-scale comparison is presented for CPR data collected in all regions and all sampling decades. More detailed analyses for the Scotian Shelf and Newfoundland Shelf regions are presented in the annual AZMP Reports from the Maritimes and Newfoundland Regions. These latter reports concentrate on data collected since 1992, since these are comparable to AZMP survey results, which date back to 1999.

Monthly average abundances ($\log_{10}(N+1)$ transformed for all but PCI1) were calculated for 15 CPR taxa by averaging values for all individual samples collected within each region for each month and year. These regional monthly average abundances were then averaged by month for samples collected within each decade prior to 2009, (i.e., 1960-1969, 1970-1979, 1980-1989, 1990-1999 and 2000-2009) to give decadal monthly average abundances, which were then averaged for each decade to give decadal annual average abundances. During the 1980s sampling was too infrequent to calculate decadal annual average abundances, except for the three regions between 30 and 45°W, and even in these regions there was no sampling in January or December. The averages of the monthly values for the 1970s and 1990s were used to fill in these missing months, however, so that decadal annual average abundances could be calculated. The averages of the decadal annual average abundances over the 4 or 5 sampling decades represent the climatological average annual abundances. Four-year annual

[1] PCI – Phytoplankton colour index, a semi-quantitative measure of total phytoplankton abundance.

average abundances were calculated for 2010-2013, using the 4-year monthly averages, and annual average abundances were calculated for 2014, where possible. According to the protocol used here, annual averages for individual years can only be calculated if there was sampling in more than 8 months, with no gaps of more than 2 consecutive months (linear interpolation being used to fill in for missing months). These criteria were met in 7 regions in 2014, for which there were 0-3 missing months, with no 2 or 3 month gaps. No annual average abundances could be calculated for the SNS region in 2014, since there was sampling in only 6 months and a 5 month gap.

Standardized abundance anomalies were calculated for the decadal (1960s, 1970s, 1980s, 1990s, 2000s), four-year (2010-2013) and annual (2014) average abundances, by subtracting the climatological average annual abundances for each time period, and by dividing the differences by the standard deviations calculated for the annual average abundances available for the individual years between 1992 and 2009. Sampling coverage was good everywhere over this period, so that annual averages could be calculated for 13-15 individual years in all regions. The underlying assumption of this approach to the calculation of the standardized abundance anomalies is that inter-annual variability was similar for all decades. This assumption was found to be reasonable for the 1960-1970s in the four regions of the sub-polar gyre, decades for which annual average abundances and standard deviations could be calculated for 15 individual years. As well, it was not inconsistent with results for the shelf regions, where annual averages over the same decades could be calculated for only 2-6 years.

The phytoplankton colour index

Climatological annual phytoplankton colour index (PCI) values (1960-2009) are highest in the two Newfoundland Shelf regions (NS, SNS), intermediate on the Scotian Shelf (WSS, ESS) and lower in the regions between 25 and 45°W (Figure 16). In the sub-polar gyre decadal average annual PCI values increased in all regions between the 1970s and 1990s and increased further thereafter, reaching record high values in 2014. In shelf regions PCI values peaked in the 1990s, dipped in the 2000s and 2010-2013, and increased in 2014.

Diatoms

Climatological annual abundances for diatoms are highest on the NS, intermediate in the SNS and ESS regions and lower in the WSS and sub-polar gyre regions (Figure 16). Decadal average annual abundances increased everywhere after the 1970s, with highest values in the 1990s (ESS) or 2000s (other regions). In 2010-2013 abundances increased in the sub-polar gyre and decreased in shelf regions, while in 2014 they were near (25-40°W, WSS), higher (NS, 40-45°W) or lower (ESS) than average.

Dinoflagellates

Climatological annual abundances for dinoflagellates are higher in shelf regions than in the sub-polar gyre. Dinoflagellate abundances increased after the 1970s with highest values in the 1990s (ESS, WSS) or 2000s (other regions) (Figure 17). In 2010-2013, dinoflagellate abundances decreased (3 regions east of 40˚W), increased (WSS) or did not change (4 other regions). In 2014 the downward trend continued in the 3 eastern regions and the upward trend continued on the WSS, while in the NS and 40-45˚W regions dinoflagellate abundances remained at the relatively high 2010-2013 levels.

Calanus I-IV

Climatological annual abundances for *Calanus* I-IV (mostly *Calanus finmarchicus*) are similar in most regions, but higher on the NS (Figure 18). In the sub-polar gyre abundances increased over the decades, peaking in 2010-2013 and decreasing in 2014. For shelf regions decadal abundance anomalies have decreased since the 1970s, except for the WSS, which shows the opposite trend (highest in the 2000s). In 2010-2013 *Calanus* I-IV abundances were close to average (NS, SNS, WSS) or lower than average (ESS), while in 2014 they were close to average.

Calanus finmarchicus V-VI

Climatological annual average abundances for *C. finmarchicus* V-VI increase slightly from east to west across the sub-polar gyre, decrease on the SNS and increase slightly farther west (Figure 18). In the 4 sub-polar gyre regions abundance anomalies have been close to average throughout the entire

sampling period. For the NS and SNS abundance anomalies were close to average until 2013, but increased on the NS in 2014. On the Scotian Shelf abundance anomalies were relatively high in the 1970s and since then have been close to average on the WSS and lower than average on the ESS, especially in 2014.

Calanus glacialis V-VI

Climatological annual abundances for *C. glacialis* are low in most regions, but higher on the NS than elsewhere (Figure 18). Decadal abundance anomalies increased slightly in all regions over the decades to maximum values in the 1990s (NS) or 2000s (other regions). In 2010-2013, *C. glacialis* abundance anomalies were close to average in all regions and in 2014 they remained near average everywhere, except for an increase on the NS.

Calanus hyperboreus III-VI

Climatological annual abundances for *C. hyperboreus* are very low in most regions, but higher on the NS than elsewhere (Figure 18). In most regions decadal abundance anomalies were close to average between the 1960s and 2000s, but in the 25-30°W region, the abundance anomaly was high in the 1970s, decreasing thereafter, with lowest values in 2010-2013 and 2014. Elsewhere abundance anomalies have remained close to average since the 2000s, although the WSS has shown an upward trend, with a relatively high value in 2014.

Small copepod taxa (Copepod nauplii, *Paracalanus/Pseudocalanus*, *Oithona* spp.)

The climatological abundances of the three small copepod groups are higher in shelf regions than in the sub-polar gyre (Figure 19). In the sub-polar gyre, decadal annual abundance anomalies for copepod nauplii and *Paracalanus/Pseudocalanus* have been higher since the 1990s than they were in previous decades, but both taxa decreased slightly in abundance in 2014. For shelf regions decadal annual abundance anomalies for copepod nauplii increased between the 1970s and 1990s and remained high (NS) or dropped to near average values in the 2000s and 2010-2013, increasing (NS, WSS) or decreasing (ESS) in 2014. *Paracalanus/Pseudocalanus* abundance anomalies in shelf regions have generally been near average, but unusually high on the NS in the 1960s and low in the SNS, ESS and WSS regions during 2010-2013 and/or 2014. Decadal annual abundances for *Oithona* spp. were generally close to average throughout all regions until the 2000s: thereafter they remained close to average in most regions, but were higher than average in the 40-45°W region in 2010-2013 and on the NS in 2014.

Macrozooplankton

Climatological annual abundances for euphausiids and hyperiid amphipods are mainly higher in the deep ocean regions of the sub-polar gyre and are highest in the 40-45°W region (Figure 20). In the sub-polar gyre euphausiid decadal abundance anomalies were generally close to average until the 2000s, but since then have been lower than average. In shelf regions euphausiid abundance anomalies have shown a downward trend since the 1970s, but with an increase to near average levels on the NS in 2014. Abundance anomalies for hyperiid amphipods increased in all regions in the 1990s compared with previous decades, although only for the NS and SNS regions were values ever very different from average during the entire 1960-2009 period, with low values on the SNS (1960s) and high values on the NS and SNS (1990s). In 2010-2013 abundance anomalies increased to higher than average values in 5 regions (2 sub-polar gyre, 3 shelf regions), while in 2014 they were lower than average in 2 sub-polar gyre regions and much higher than average in shelf regions.

Acid-sensitive taxa

Coccolithphores, phytoplankton that are covered with calcite scales, and foraminifera (forams) whose shell composition includes calcium carbonate, have been counted in CPR samples only since 1991. Coccolithophores are generally less abundant on the NS and Scotian Shelf than elsewhere and forams are more abundant in the sub-polar gyre than in shelf regions (Figure 21). Changes in coccolithophore abundance may be linked to changes in stratification (Raitsos et al. 2006). Both taxa were generally more abundant in 2010-2013 than before and both remained at high levels in 2014 in the regions between 40°W and the ESS. Elsewhere abundance anomalies for both taxa were generally near average in 2014, except for high values for coccolithphores in the 30-35°W region and for forams on

the WSS. Pteropods of the genus *Limacina* have shells that are composed of aragonite, which is a form of calcium carbonate that is especially sensitive to dissolution at low pH. Climatological annual abundances for *Limacina* show a more-or-less flat distribution across all regions. Over the decades *Limacina* abundance anomalies have generally been close to average, but in 2010-2013 they were higher than average in the NS and WSS regions, remaining high on the NS in 2014. Elsewhere abundance anomalies were close to average in 2014.

Summary

The Atlantic Zone Off-Shelf Monitoring Program (AZOMP) provides observations on ocean climate and plankton variability affecting regional climate and ecosystems off Atlantic Canada and the global climate system. The reporting year however possessed a challenge to us with the unavailability of a suitable oceanographic research vessel. Because of that it was not possible to carry out our regular field campaign resulting in limited data from the chemistry and biology realms, and therefore making us to rely exclusively on profiling float, remote-sensed and atmospheric reanalysis data, and ocean model simulation products.

In the Labrador Sea, surface heat losses in winter result in the formation of dense waters, which spread across the ocean ventilating its deep layers and essentially driving the global ocean overturning circulation. In the winter of 2016-17, as in the previous winter, the mid-high latitude North Atlantic experienced more moderate surface heat loss than in the winter of 2014-15 which in its time produced the highest heat losses in more than two decades. Despite the weaker heat loss from the ocean to the atmosphere in the winters of 2015-16 and 2016-17, the water column preconditioning staged by convective mixing in the previous years led nevertheless to the most significant formation, in terms of volume and depth, of Labrador Sea Water (LSW) since 1994. Similarly to 2016, the temperature and salinity profiles obtained by the Argo floats in 2017 show that the winter mixed layer and hence convection in the central Labrador Sea penetrated below 2000 m in the reporting year, exceeding the mixed layer depths of 1600, 1700 and 1850 m in 2014, 2015 and 2016, respectively. The 2017 vintage of LSW is associated with low temperature (<3.3°C) and salinity (<34.86) between 1000 and 1700 m. The winter convection in 2016 and especially the one in 2017 are arguably the deepest since the record of 2500 m in 1994, and the resulting LSW year class is one of the largest ever observed outside of the early 1990s. This also suggests that the strong winter convection in 2017 further added to increased gas (dissolved oxygen, anthropogenic gases, and carbon dioxide) uptakes and consequently respective gas concentrations in the Labrador Sea in the lower part of the 0-2000 m layer, but this could not be confirmed from direct ship-based measurements.

In order to be able to measure the ocean colour using satellite imagery, you need a cloud-free sky. The Labrador Sea region tends to be generally cloudy, particularly in the spring. In fact, over a period of five weeks running form end of April to early June of 2017, the percent coverage in the central region never exceeded 20% in any seven-day composite, and most of the good pixels were provided by the northeast corner of the box. Missing an important portion of the bloom initiation phase, it makes it nearly impossible to estimate its magnitude. In both inshore regions a bloom onset happened earlier than usually in 2017, but while the bloom did persist in its duration on the Greenland Shelf helping to bring the magnitude to relatively high values, the situation was reversed on the Labrador Shelf resulting in a relatively lower than average phytoplankton bloom.

As a result of the cancellation of the spring research survey, we were not able to update the rate of decline in pH, previously reported as -0.002 y^{-1} for the 1994-2016 period, nor was it possible to assess the state of *Calanus finmarchicus*, the dominant mesozooplankton in the western and central region of the Labrador Sea, following the record lows reported in 2016.

Acknowledgements

We would like to thank #### for his helpful comments and suggestions. The NCEP Reanalysis data were provided by the NOAA-CIRES Climate Diagnostics Center, Boulder, Colorado, USA. The sea ice concentration anomaly data are the US National Snow and Ice Data Center.

References

Brickman, D., Z. Wang, and B. Detracy (2015), Variability of Current Streams in Atlantic Canadian Waters: A Model Study. Atmosphere and Ocean. doi:10.1080/07055900.2015.1094026

Wang Z. , D. Brickman, B. Greenan and I. Yashayaev (2016), An abrupt shift in the Labrador Current System in relation to winter NAO events. Journal of Geophysical Research: Oceans. DOI: 10.1002/2016JC011721.

Fragoso, Glaucia M., Alex J. Poulton, Igor M. Yashayaev, Erica J.H. Head, Mark C. Stinchcombe, and Duncan A. Purdie. Biogeographical Patterns and Environmental Controls of Phytoplankton Communities from Contrasting Hydrographical Zones of the Labrador Sea. Progress in Oceanography 141 (February 2016): 212–26. doi:10.1016/j.pocean.2015.12.007.

Azetsu-Scott, K., A. Clarke, K. Falkner, J. Hamilton, E. P. Jones, C. Lee, B. Petrie, S. Prinsenberg, M. Starr and P. Yeats (2010), Calcium Carbonate Saturation States in the waters of the Canadian Arctic Archipelago and the Labrador Sea, 115, C11021, doi:10.1029/2009JC005917 Journal of Geophysical Research.

Barnston, A. G., and R. E. Livezey (1987), Classification, seasonality and persistence of low-frequency atmospheric circulation patterns. Mon. Wea. Rev., 115, 1083-1126.

Caldeira, K., and M. E. Wickett (2003), Anthropogenic carbon and ocean pH, Nature, 425, 365

Climate Prediction Center (2010), NOAA/National Weather Service, National Centers for Environmental Prediction. Camp Springs, MA. http://www.cpc.noaa.gov/products/precip/CWlink/daily_ao_index/ao.shtml#publication

Egge, J., and Aksnes, D.L. (1992), Silicate as regulating nutrient in phytoplankton competition. Mar. Ecol. Prog. Ser. **83**(2-3): 281–289. doi: 10.3354/meps083281.

Fetterer, F., K. Knowles, W. Meier, and M. Savoie (2002), updated 2011. Sea ice index. Boulder, CO: National Snow and Ice Data Center. Digital media.

Feely, R. A., C. L. Sabine, K. Lee, W. Berelson, J. Kleypas, V. J. Fabry,and F. J. Millero (2004), Impact of anthropogenic CO_2 on the $CaCO_3$system in the oceans, Science, 305, 362–366.

Fragoso, G.M., Poulton, A.J., Yashayaev, I.M., Head, E.J.H., Stinchcombe, M.C., and Purdie, D.A. 2016. Biogeographical patterns and environmental controls of phytoplankton communities from contrasting hydrographical zones of the Labrador Sea. Progress in Oceanography 141: 212–226. doi:10.1016/j.pocean.2015.12.007.

Harrison, W.G. and W.K.W. Li (2008), Phytoplankton growth and regulation in the Labrador Sea: light and nutrient limitation. J. Northwest. Atl. Fish. 39:71-82.

Hauser, T., Demirov, E., Zhu, J. and I Yashayaev (2015), North Atlantic atmospheric and ocean inter-annual variability over the past fifty years – Dominant patterns and decadal shifts. Progress in Oceanography, Volume 132, March 2015, Pages 197–219

Head, E.J.H., Harris, L.R and I Yashayaev. (2003), Distributions of *Calanus* spp. and other mesozooplankton in the Labrador Sea in relation to hydrography in spring and early summer (1995-2000). Prog. Oceanogr. 59: 1-30

Hurrell, J. W. (1995), Decadal trends in the North Atlantic Oscillation: Regional temperatures and precipitation. Science, 269, 676-679.

Josey, S., J. Grist, D. Kieke, I. Yashayaev, and L. Yu (2015), Sidebar: Extraordinary ocean cooling and new dense water formation in the North Atlantic [in "State of the Climate 2014"], Bull. Amer. Meteor. Soc.

Kalnay, E., M. Kanamitsu, R. Kistler, W. Collins, D. Deaven, L. Gandin, M. Iredell, S. Saha, G. White, J. Woollen, Y. Zhu, M. Chelliah, W. Ebisuzaki, W. Higgins, J. Janowiak, K.C. Mo, C. Ropelewski, J. Wang, A. Leetmaa, R. Reynolds, R. Jenne, and D. Joseph (1996), The NCEP/NCAR 40-Year Reanalysis Project., Bull. Amer. Meteor. Soc., 77, No. 3, 437-470.

Li, W.K.W. and W.G. Harisson, 2014, The state of phytoplankton and bacterioplankton and bacterioplankton in the Labrador Sea: Atlantic Zone Off-Shelf Monitoring Program 1994-2013. Can. Tech. Rep. Hydrogr. Ocean. Sci. 302:xviii+181p.

Raitsos, D.E., Lavender, S.J., Pradhan, Y., Tyrrell, T., Reid, P.C., Edwards, M. (2006), Coccolithophore bloom size variation in response to the regional environment of the subarctic North Atlantic. Limnol. Oceanogr. 51: 2122-2130.

Rey, F. (2012), Declining silicate concentrations in the Norwegian and Barents Seas. ICES J. Mar. Sci. J. Cons. **69**(2): 208–212

Richardson, A.J., Walne, John, A.W.G., Jonas, T.D., Lindley, J.A., Sims, D.W., Stevens, D. and M. Witt, (2006), Using continuous plankton recorder data. Prog. Oceanogr. 68: 27-74.

Thornalley D.J.R., D.W. Oppo, P. Ortega, J.I. Robson, C.M. Brierley, R. Davis, I.R. Hall, P. Moffa-Sanchez, N.L. Rose, P.T. Spooner, I. Yashayaev, L.D. Keigwin., (2018), Anomalously weak Labrador Sea convection and Atlantic overturning during the past 150 years. Nature, 2018; 556 (7700): 227 DOI: 10.1038/s41586-018-0007-4

Visbeck, M.H., J.W. Hurrell, L. Polvani and H.M. Cullen (2001), The North Atlantic Oscillation: Past, Present and Future. Proc. Nat. Acad. Sci., 98, 12876-12877 doi: 10.1073/pnas.231391598

Yashayaev, I. (2007), Hydrographic changes in the Labrador Sea, 1960-2005, Progress in Oceanography, 73, 242-276.

Yashayaev, I., and J.W.Loder (2009), Enhanced production of Labrador Sea Water in 2008. Geophys. Res. Lett., 36: L01606, doi:10.1029/2008GL036162.

Yashayaev, I., and J.W.Loder (2016), Recurrent replenishment of Labrador Sea Water and associated decadal-scale variability. Journal of Geophys. Res.: Oceans, 121, 11, DOI: 10.1002/2016JC012046.

Yashayaev, I., and J.W.Loder (2017). Further intensification of deep convection in the Labrador Sea in 2016. Geophysical Research Letters, 44, 3, DOI: 10.1002/2016GL071668.

Yebra, L., Harris, R.P., Head, E.J.H., Yashayaev, I., Harris, L.R., and Hirst, A.G. (2009). Mesoscale physical variability affects zooplankton production in the Labrador Sea. Deep Sea Research Part I: Oceanographic Research Papers 56(5): 703–715.

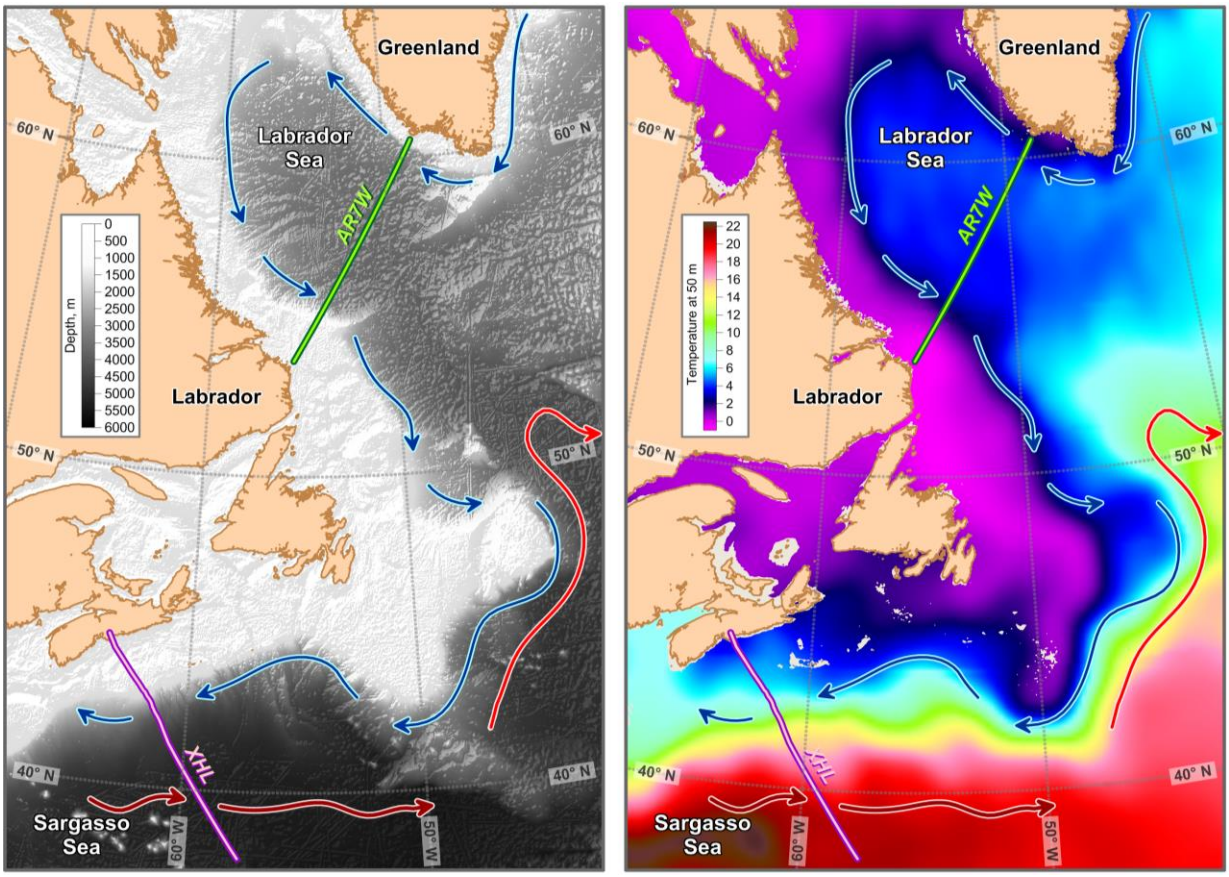

Figure 1. Major topographic and ocean circulation features in the AZMP/AZOMP domain. The AR7W and Extended Halifax (XHL) lines indicated in the map along with respective sampling locations/sites form a core component of the DFO Atlantic Zone Offshore Monitoring Program (AZOMP). Arbitrary coordinate boxes used for averaging the remote-sensed ocean color and sea surface temperature measurements are shown in blue for the Labrador Shelf, red for the Labrador Basin and green for the Greenland Shelf and in black for the Central Region.

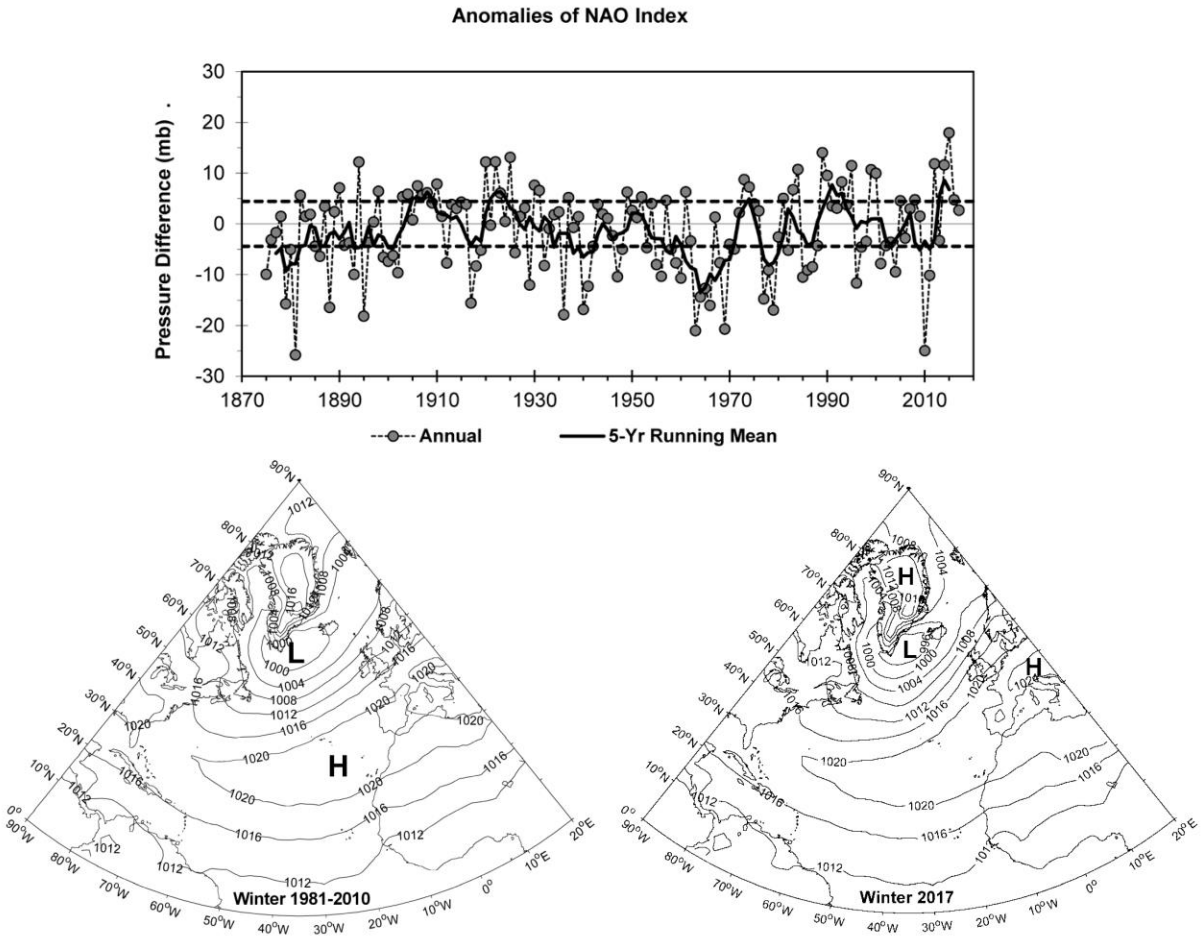

Figure 2. Anomalies of the North Atlantic Oscillation (NAO) index, defined as the winter (December, January, February) sea level pressure difference between the Azores and Iceland, relative to the 1981-2010 mean. The 0.5 (green broken lines) and 1.0 (red broken lines) standard deviations (SDs) are shown (upper panel). The lower panels show the 1981-2010 December-February all-winter mean (bottom left) and 2016-2017 December-February single-winter mean (bottom right) sea level pressure over the North Atlantic.

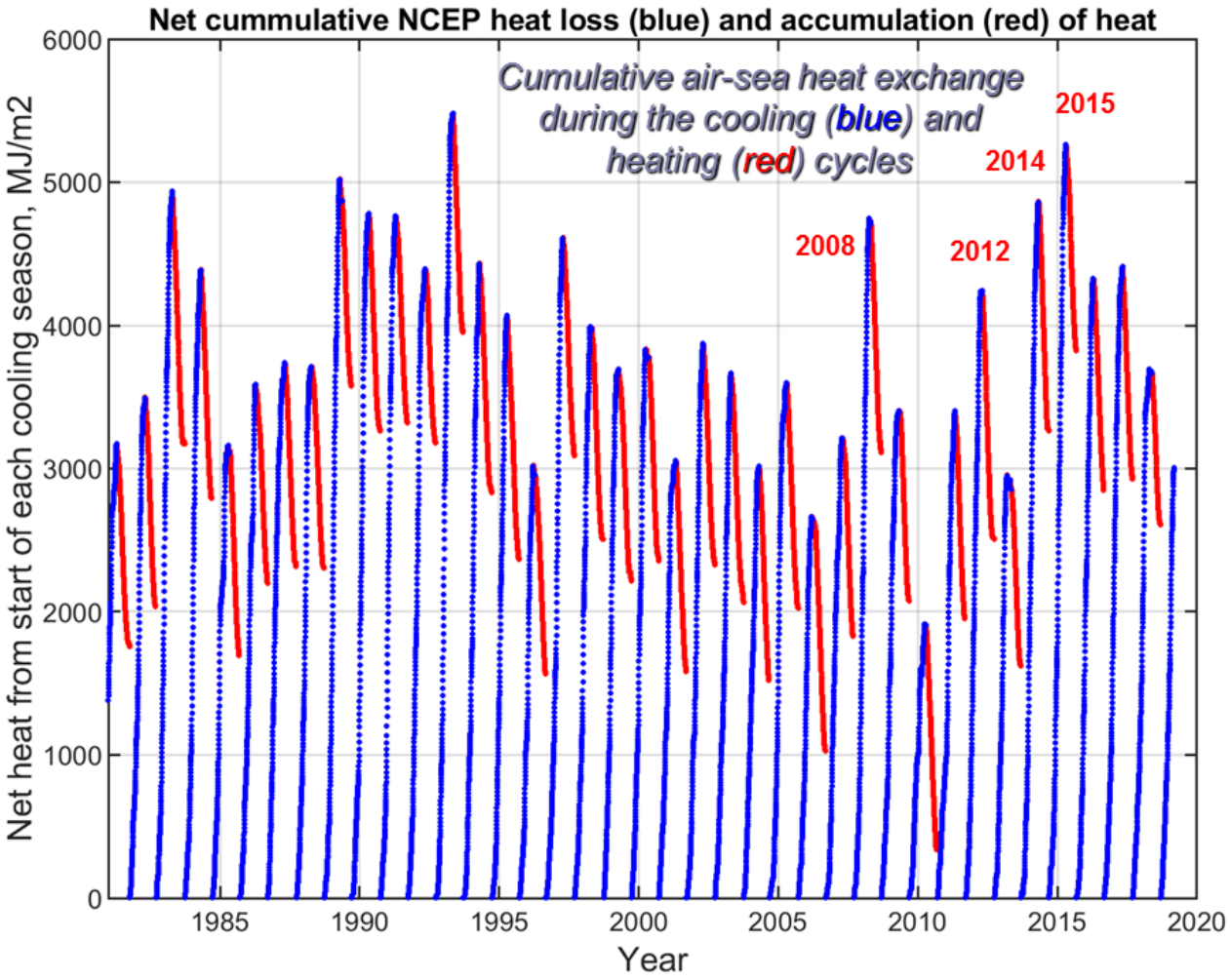

Figure 3. Sea surface heat losses/gains (blue/red) integrated over individual cooling/heating seasons in the central region Labrador Sea. The net heat flux values unsed in this intergration were computed as a sum of incoming and outgoing short and long wave readiation, latent and sinsible heat fluxes based on the NCEP/NCAR reanalysis fields. The years of high surface heat losses recorded in the Labrador Sea over the past ten years are indicated with red circles.

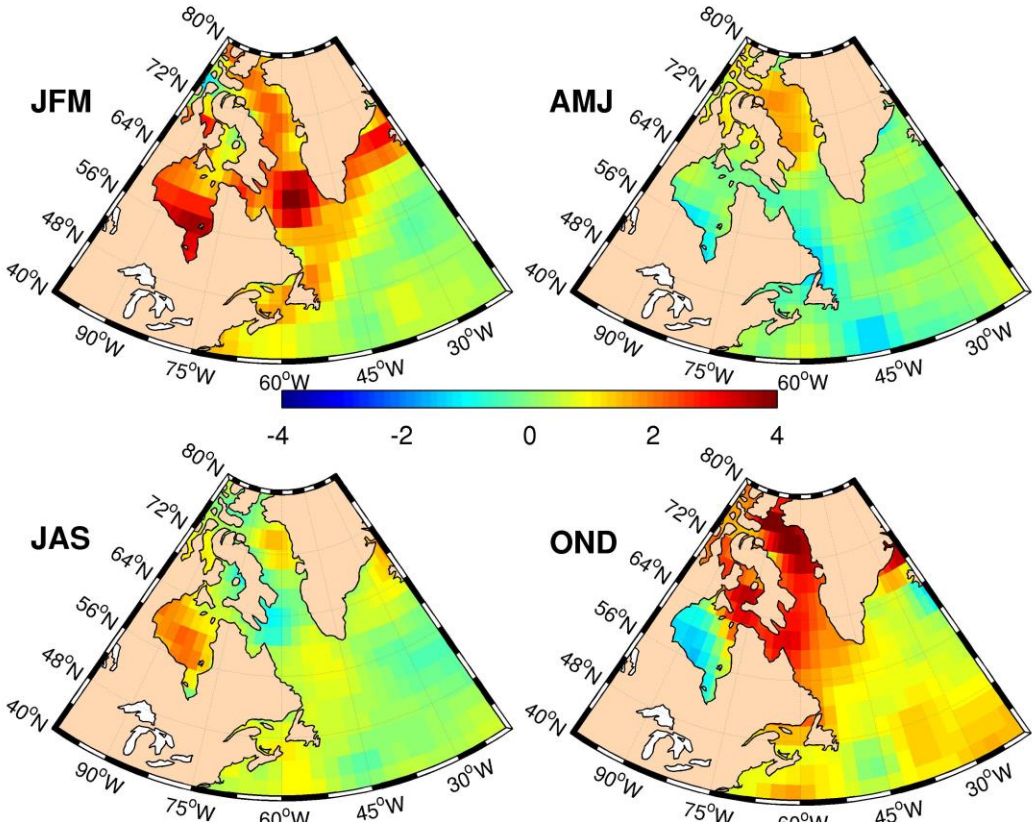

Figure 4. Surface air temperature anomaly for winter, spring, summer and fall periods in 2017 as derived from NCEP/NCAR reanalysis. http://www.esrl.noaa.gov/psd/

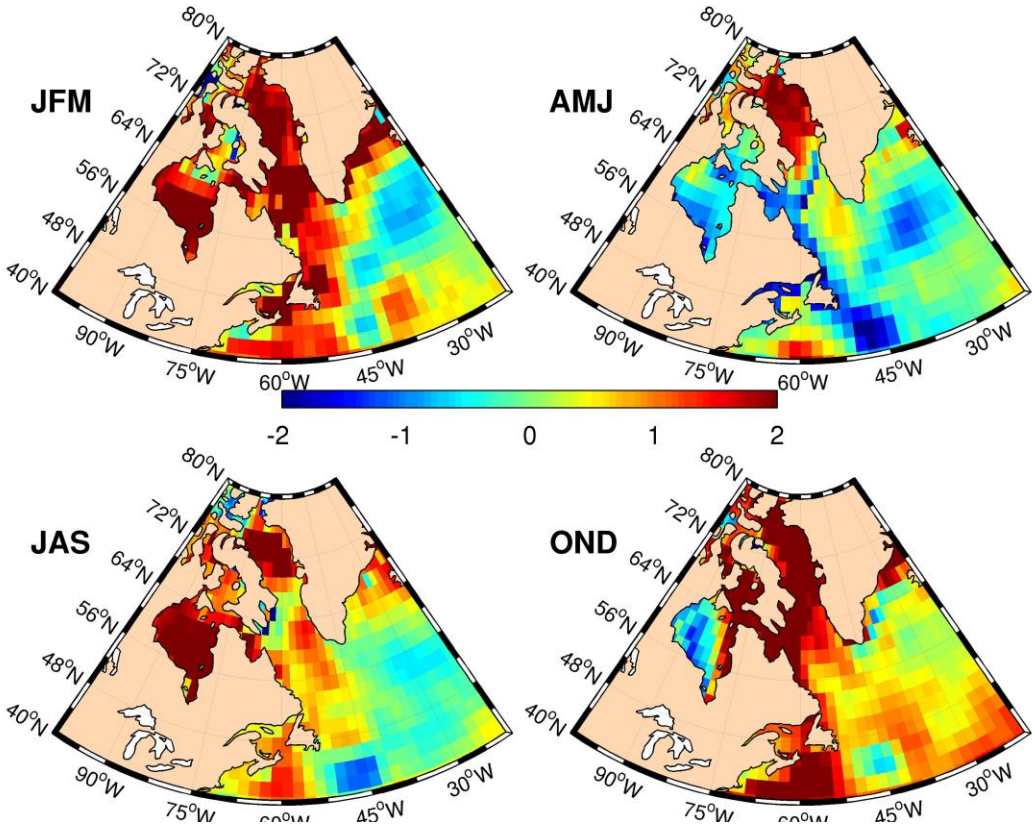

Figure 5. Sea surface temperature anomaly for winter, spring, summer and fall periods in 2017 as derived from ERSST and spring, summer and from NCEP/NCAR reanalysis. http://www.esrl.noaa.gov/psd/.

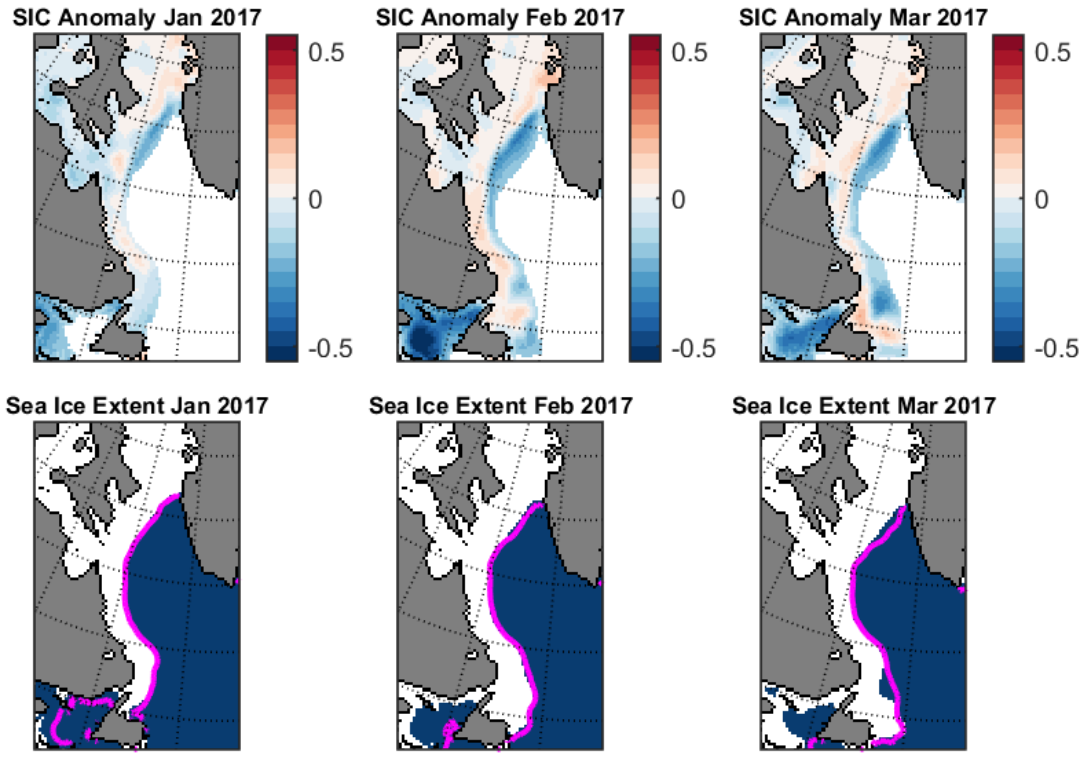

Figure 6. Sea ice concentration anomalies (top) and sea ice extent (bottom) for January-March 2017 as derived by the US National Snow and Ice Data Center (reference period 1979-2000) http://nsidc.org/.

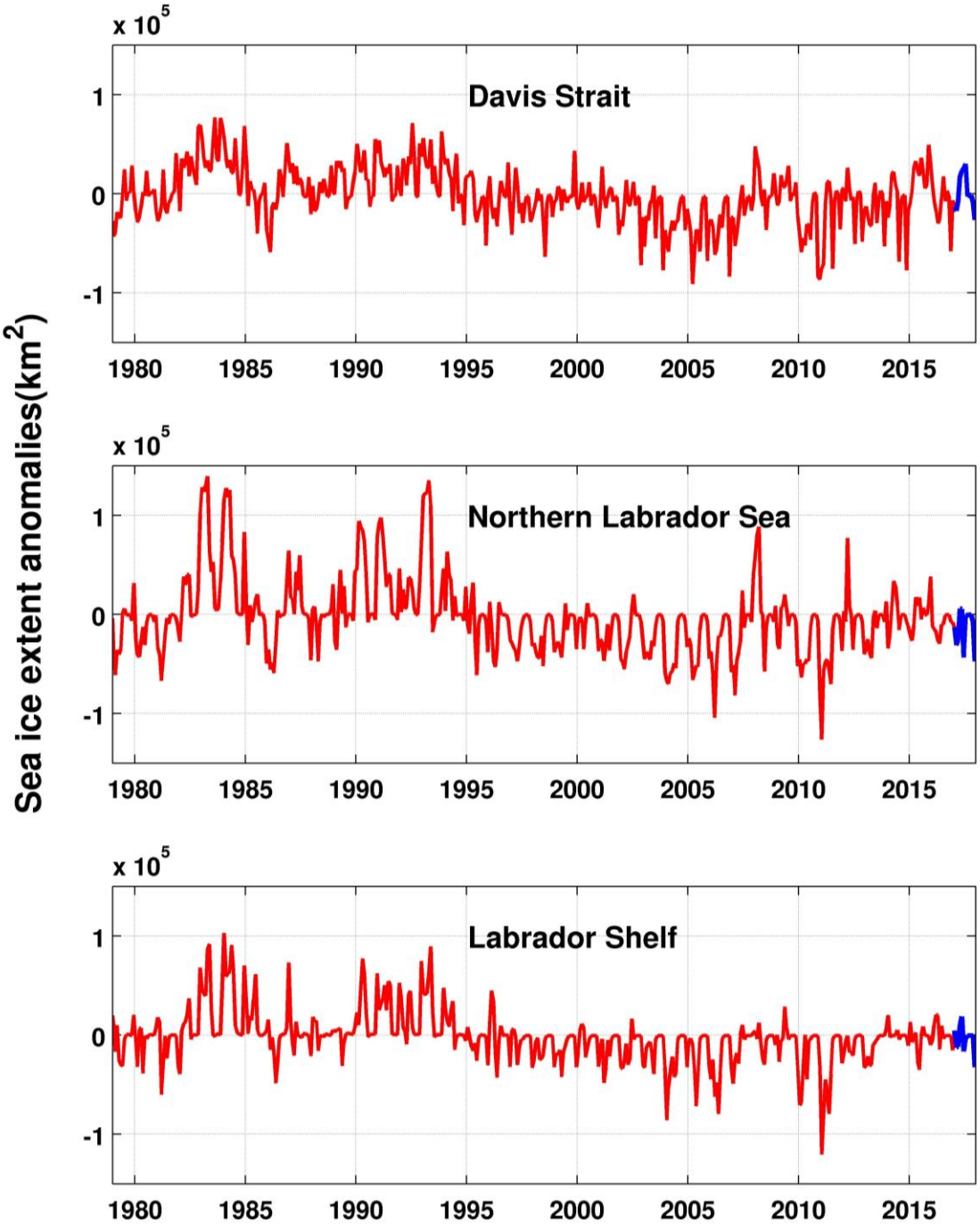

Figure 7. The computed monthly sea ice extent anomalies for Davis Strait area, northern Labrador Sea, and Labrador Shelf, based on ice concentration data from the US National Snow and Ice Data Center (reference period 1981-2010). http://nsidc.org/data/ .

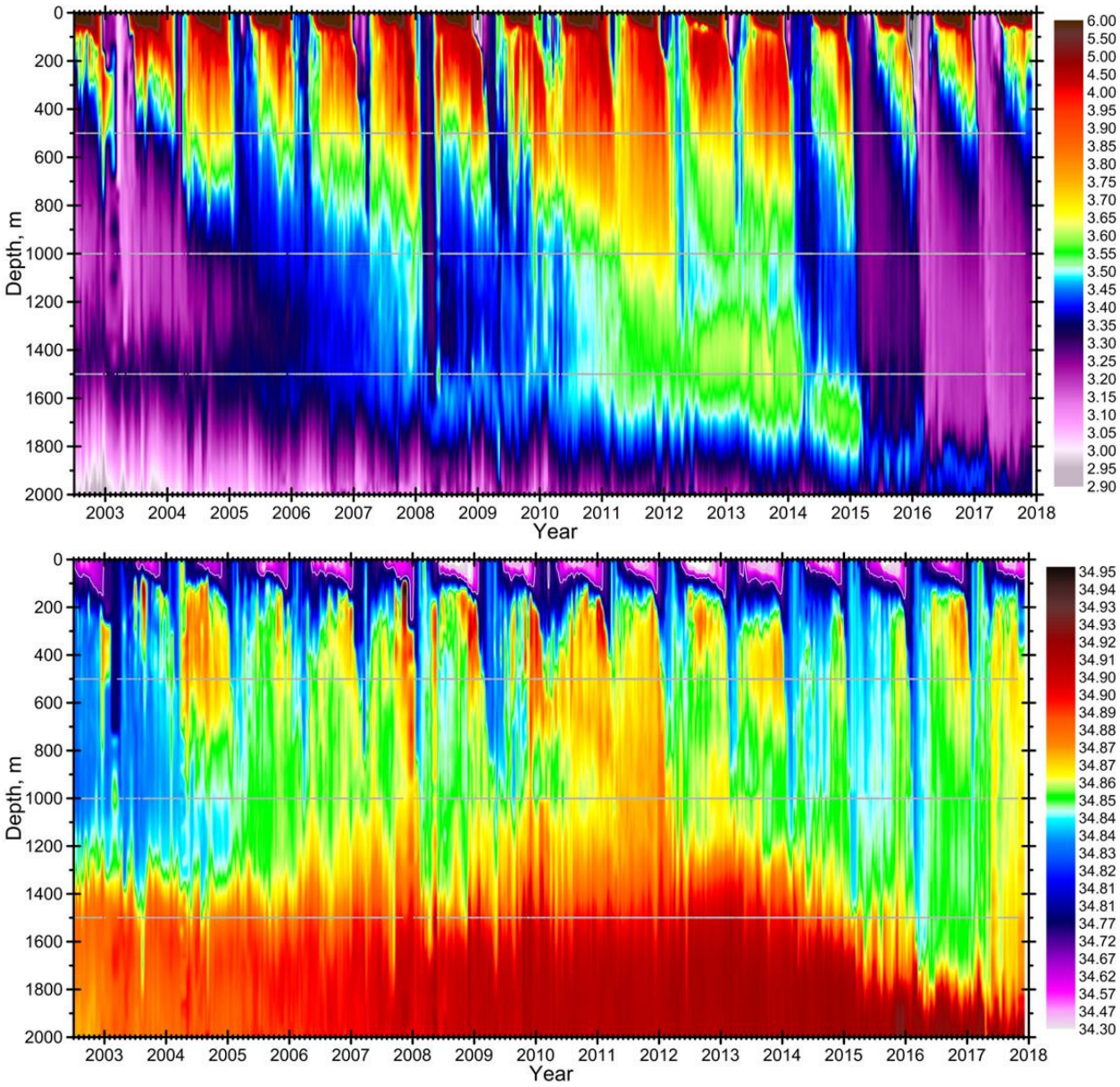

Figure 8. Variability of temperature (upper panel) and salinity (lower panel) in the central region of the Labrador Sea based on profiling Argo float and research vessel survey data from 0 to 2000 m for the time period of 2002-2018.

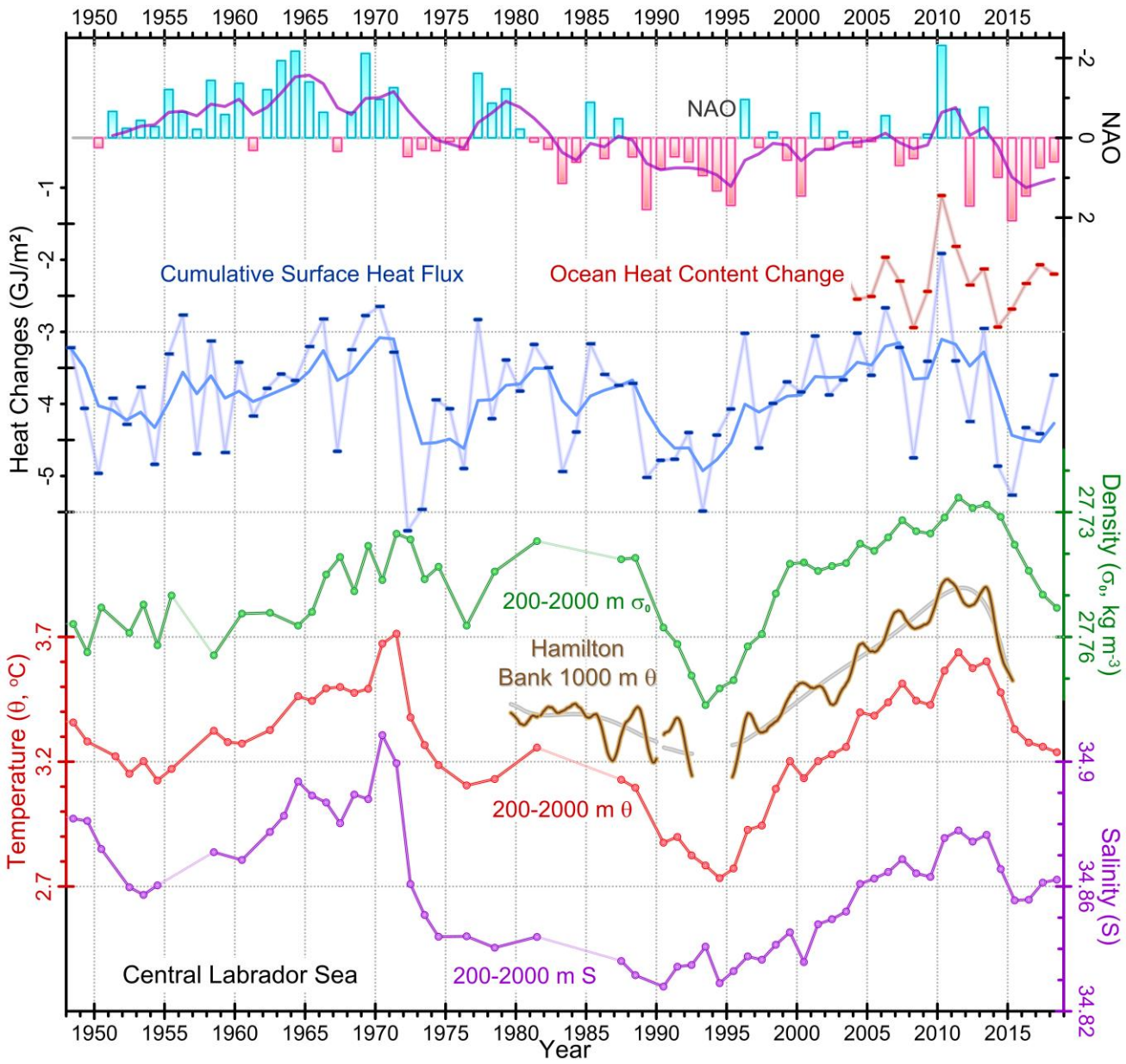

Figure 9. Key climatic indices for the central Labrador Sea since 1948. The upper bar graph shows the normalized winter NAO index (inverted scale). The next two time series represent heat changes in the central Labrador Sea during each yearly cooling season: first, the change in ocean heat content during each ocean cooling season of the Argo era (2003-present; providing all-season data coverage) based on temperature profiles (red), and, second, the change inferred from the cumulative surface heat flux computed from National Centers for Environmental Prediction (blue) and the value a five-point filter (solid line with value plotted at the last year of each period).The lower four curves are estimates of the annual density (σ_0, referenced to the surface; inverted scale), mean temperature (θ) and salinity (S) averaged over the 200–2000 m interval in the central Labrador Sea, and temperature from near-bottom current meter at about/approximately 1000 m depth east of Hamilton Bank.

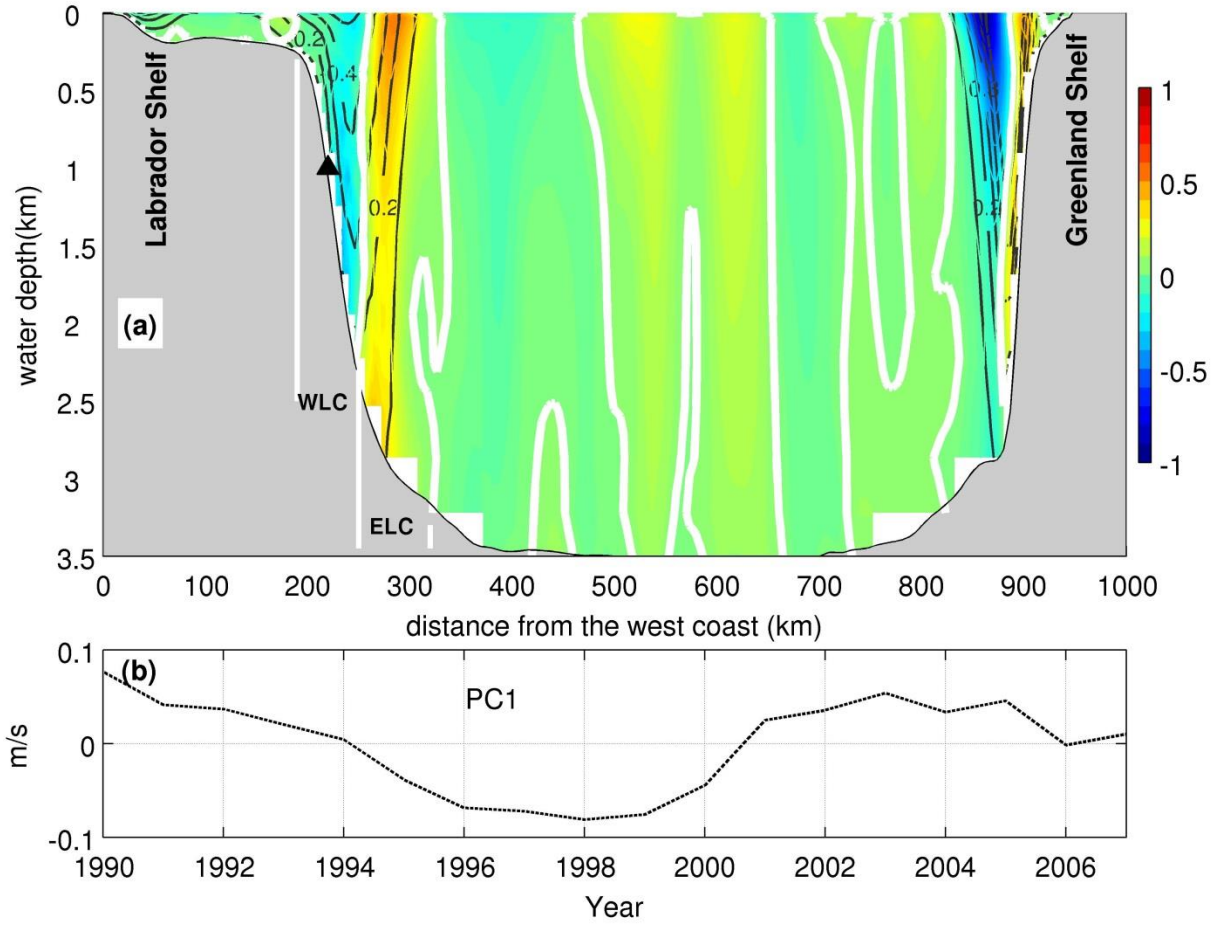

Figure 10. (a) EOF1 pattern of the normal velocities along AR7W (based on BNAM simulations for 1990-2007). The shading represents the EOF values demarcated by the zero EOF contours shown as the bold white lines. The black labeled contours represent the mean normal velocities (in m/s). Note that the positive values represent the northward flow. The black triangle indicates the location of the mooring referred to in the text. (b) Corresponding EOF1 loadings known as PC1.

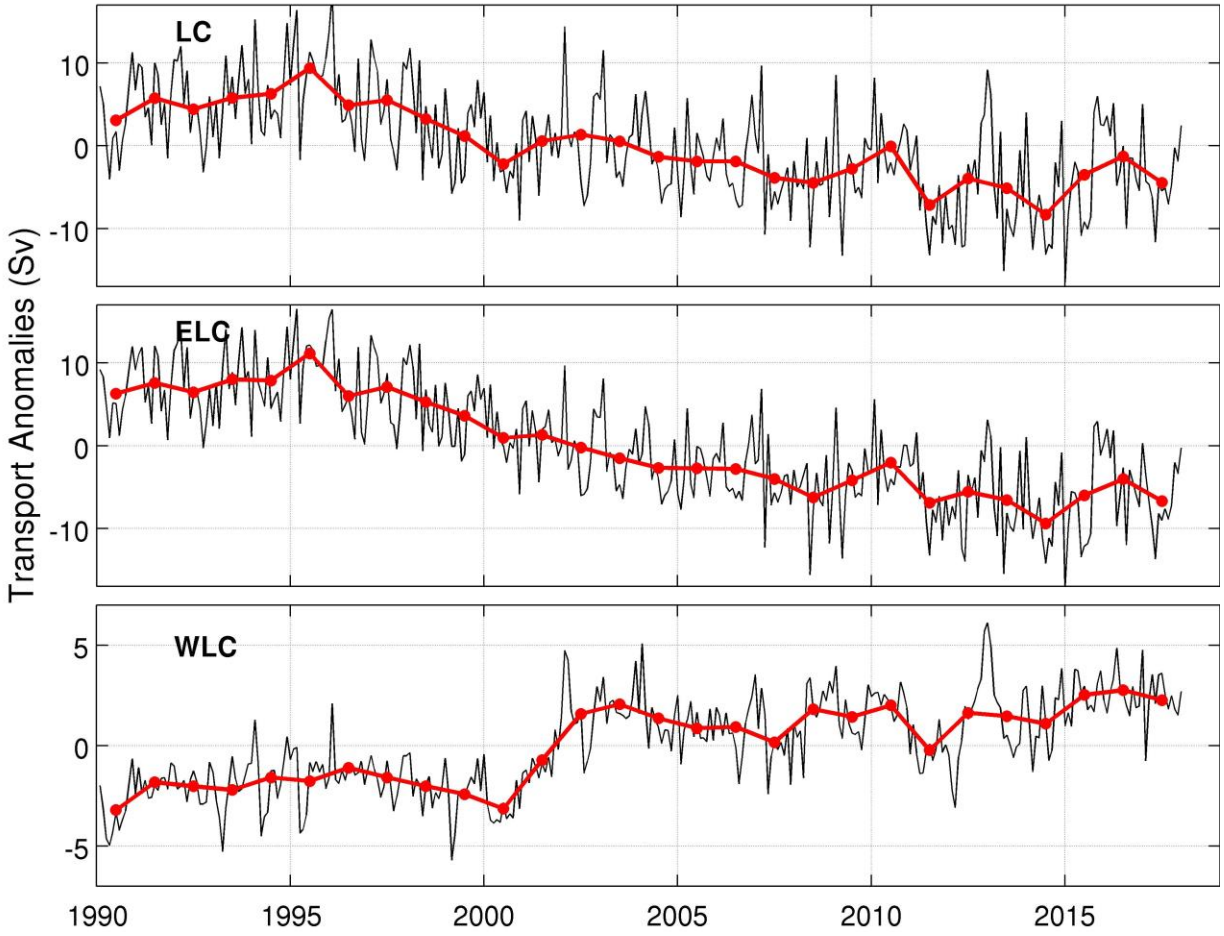

Figure 11. Transport anomalies of the LC, ELC, and WLC from 1990 to 2017. Note that the black lines connect the monthly data, and the dots connected by the red lines represent the annual means.

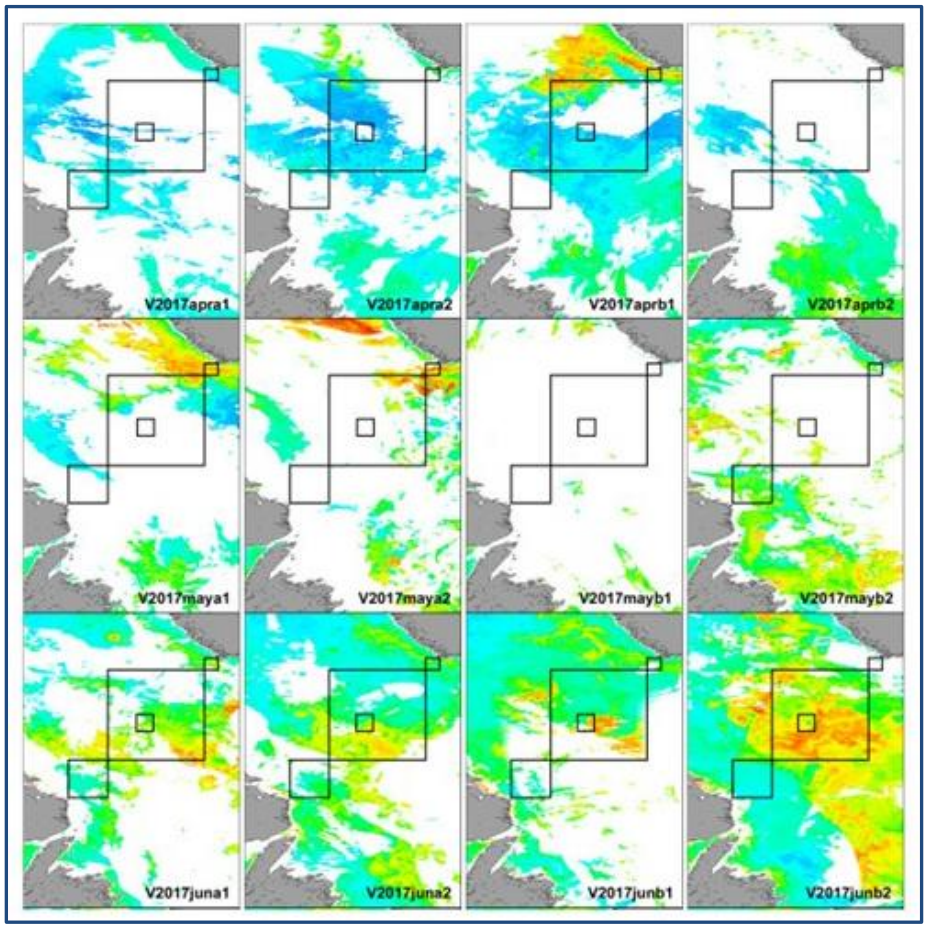

Figure 12. 2017 April to June weekly ocean colour composite for the central and southern Labrador Sea area. The black boxes indicate the regions used for averaging of remote-sensed data presented in the time series in Figure 13.

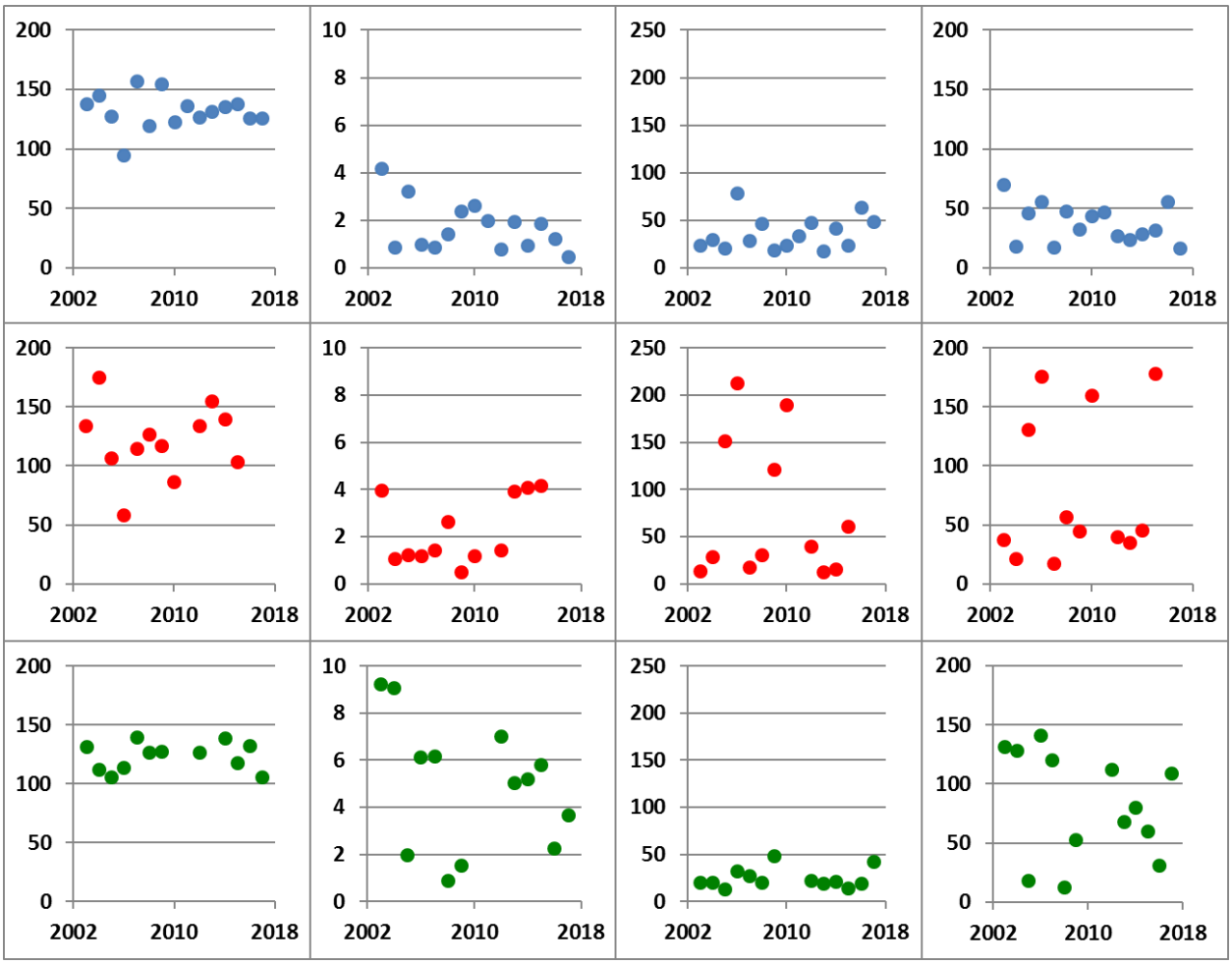

Figure 13. Phytoplankton bloom characterisation using fitted Gaussian curve to define the start of the bloom on the left, its amplitude (mg/m^3) second from the left, its duration in number of days third from the left and its magnitude corresponding to the area under the curve on the right (Zhai et al., 1991) in the Labrador Shelf, Central Basin and Greenland Shelf domains indicated by the three boxes in Figure 12.

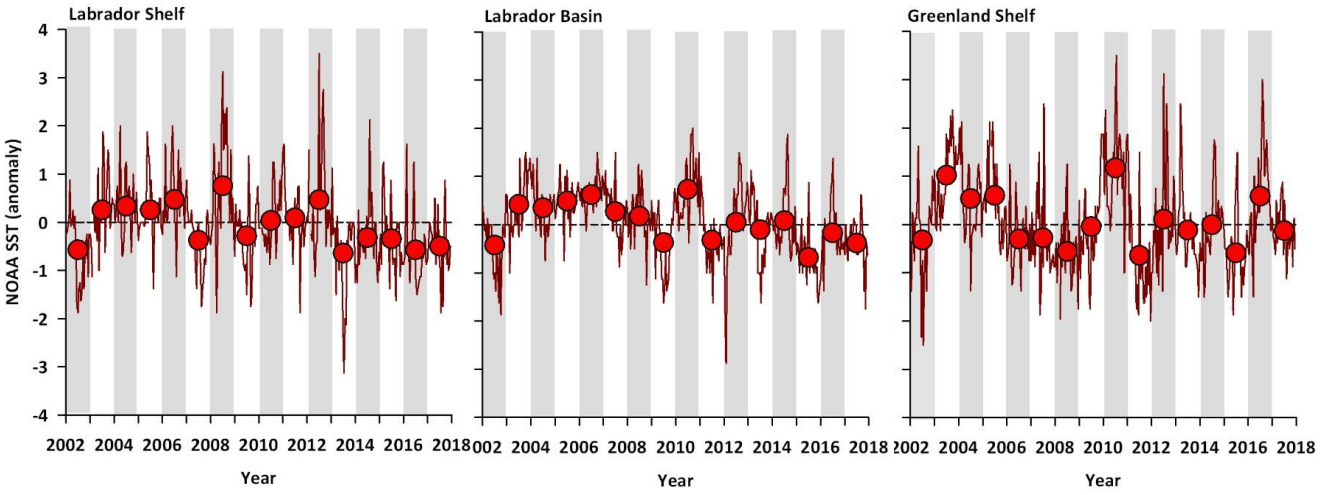

Figure 14. SST anomaly time series (2002-2018) for Labrador Shelf (left column), Labrador Basin (middle column) and Greenland Shelf (right column) estimated from bi-weekly AVHRR data. Lines represents biweekly anomalies, circles indicates annual average anomalies.

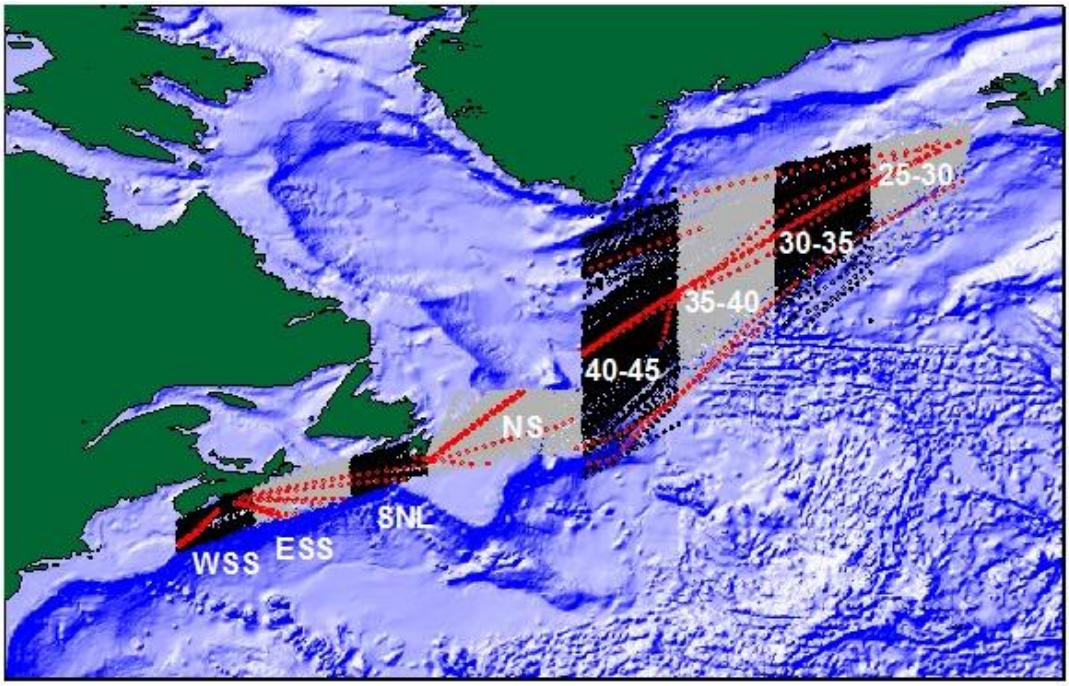

Figure 15. Continuous Plankton recorder (CPR) lines and stations 1957 to 2015. Stations sampled in 2015 are shown in red. Data are analysed by region. Regions are: Western Scotian Shelf (WSS), Eastern Scotian Shelf (ESS), South Newfoundland Shelf (SNL), Newfoundland Shelf (NS), and between longitudes 40-45°W, 35-40°W, 30-35°W, 25-30°W.

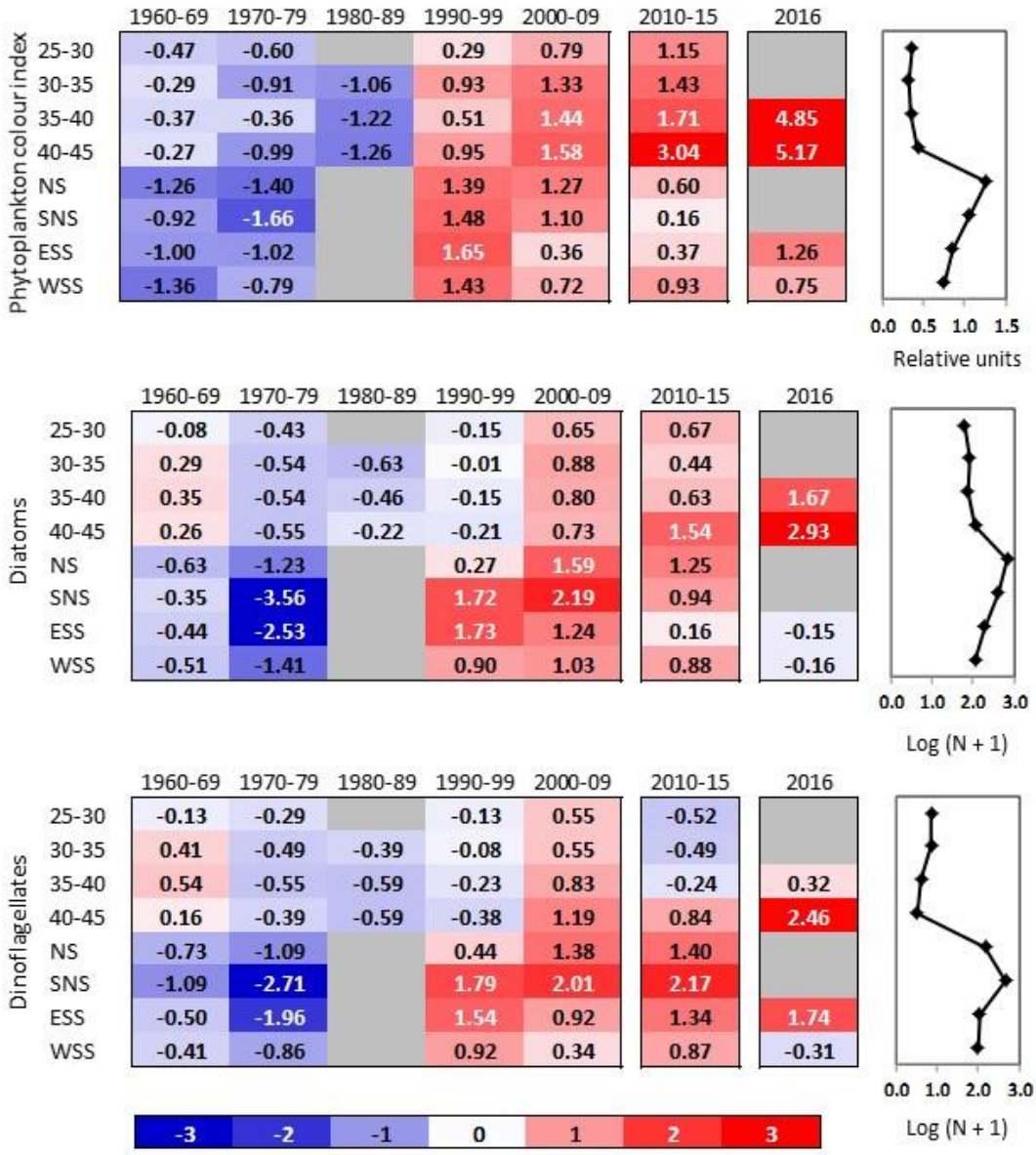

Figure 16. Scorecards for long-term (1960-2016) CPR time series for three indices of phytoplankton concentration in eight regions of the NW Atlantic. Standardised anomalies were calculated using annual averages calculated from monthly averages over decadal (1960-2009), 6 year (2010-2015) or annual (2016) periods, based on climatological averages calculated for the decadal annual averages between 1960 and 2009 (shown in the panels on the right) and standard deviations calculated for the years 1992-2009. Blank cells correspond to years (decades) when sampling was too sparse to give annual (decadal) values. Red (blue) cells indicate higher (lower) than normal values. The numbers in the cells are the standardised anomalies. The regions are: Western Scotian Shelf (WSS), Eastern Scotian Shelf (ESS), South Newfoundland Shelf (SNL), Newfoundland Shelf (NS), and between longitudes 40-45°W, 35-40°W, 30-35°W, 25-30°W.

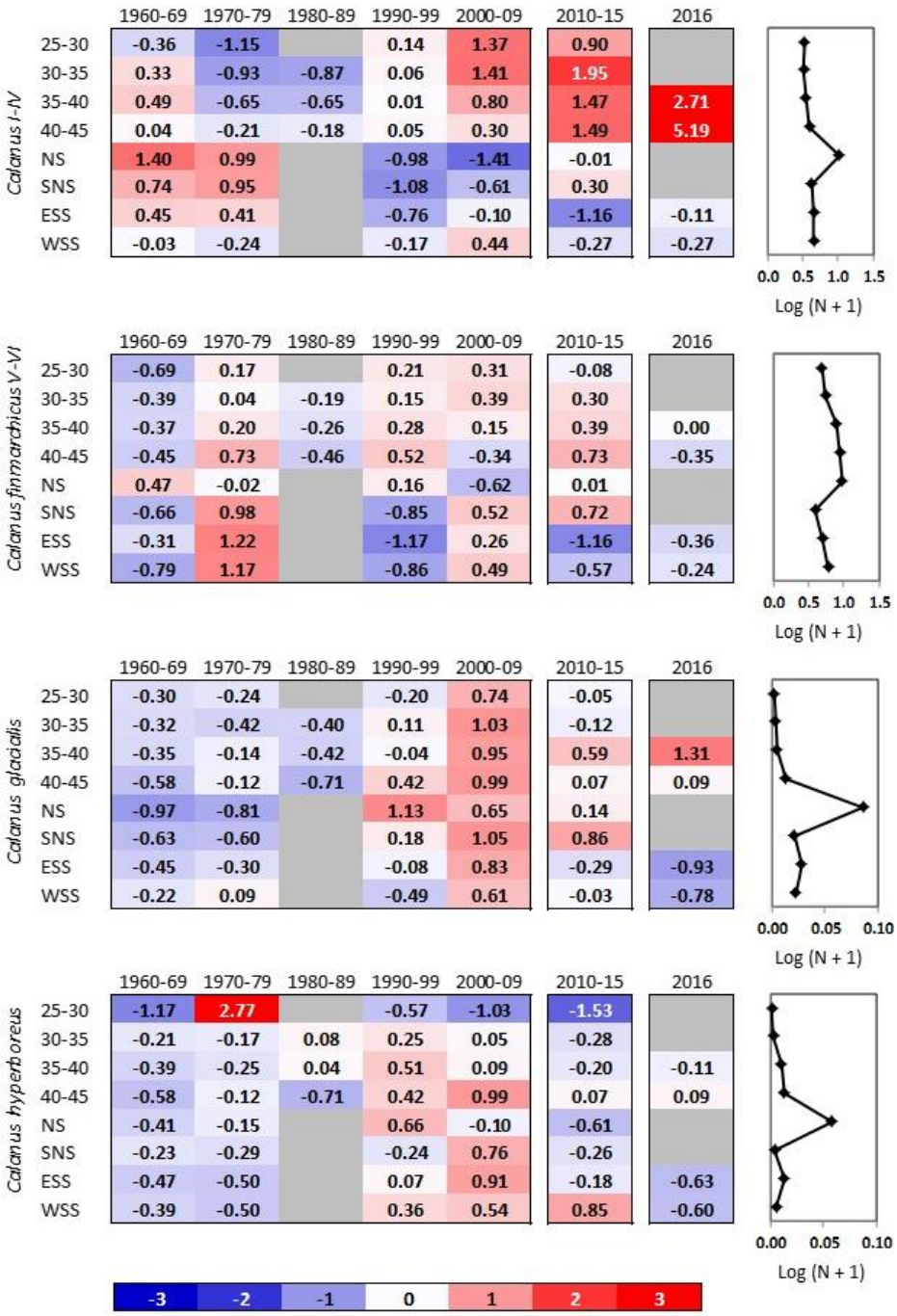

Figure 17. Scorecards for short-term (1994-2016) CPR time series for three indices of phytoplankton concentration in eight regions of the NW Atlantic. Standardised annual anomalies were calculated using annual averages, calculated from monthly averages, based on climatological averages and standard deviations for the 1994-2012 period, shown on the right. Blank cells correspond to years when sampling was too sparse to give annual values. Red (blue) cells indicate higher (lower) than climatological values. The numbers in the cells are the standardised anomalies. The regions are: Western Scotian Shelf (WSS), Eastern Scotian Shelf (ESS), South Newfoundland Shelf (SNL), Newfoundland Shelf (NS), and between longitudes 40-45°W, 35-40°W, 30-35°W, 25-30°W.

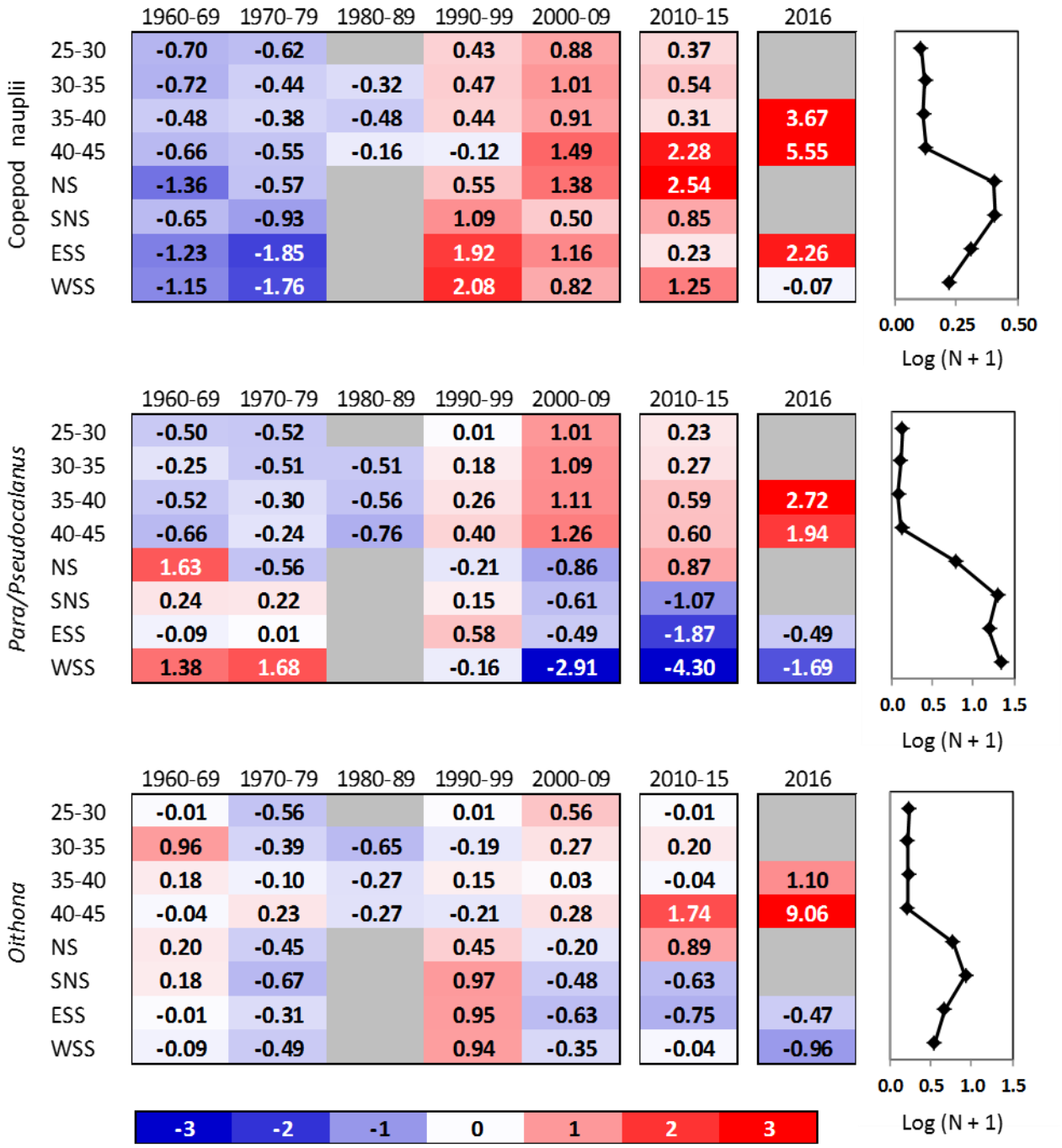

Figure 18. Scorecards for long-term (1960-2016) CPR time series for three small copepod taxa in eight regions in the NW Atlantic. Details as in Figure 16.

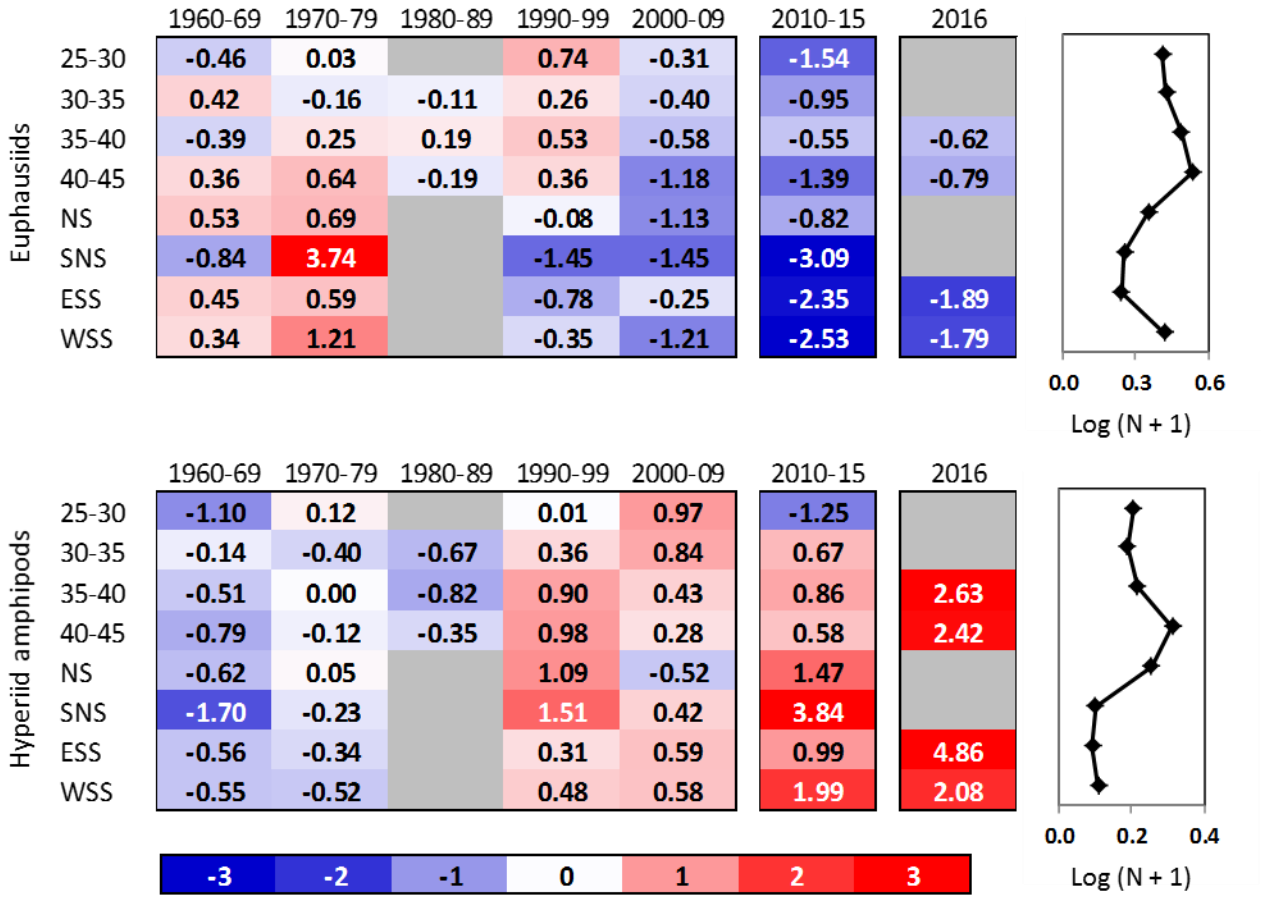

Figure 19. Scorecards for long-term (1960-2016) CPR time series for two macrozooplankton taxa in eight regions in the NW Atlantic. Details as for Figure 16.

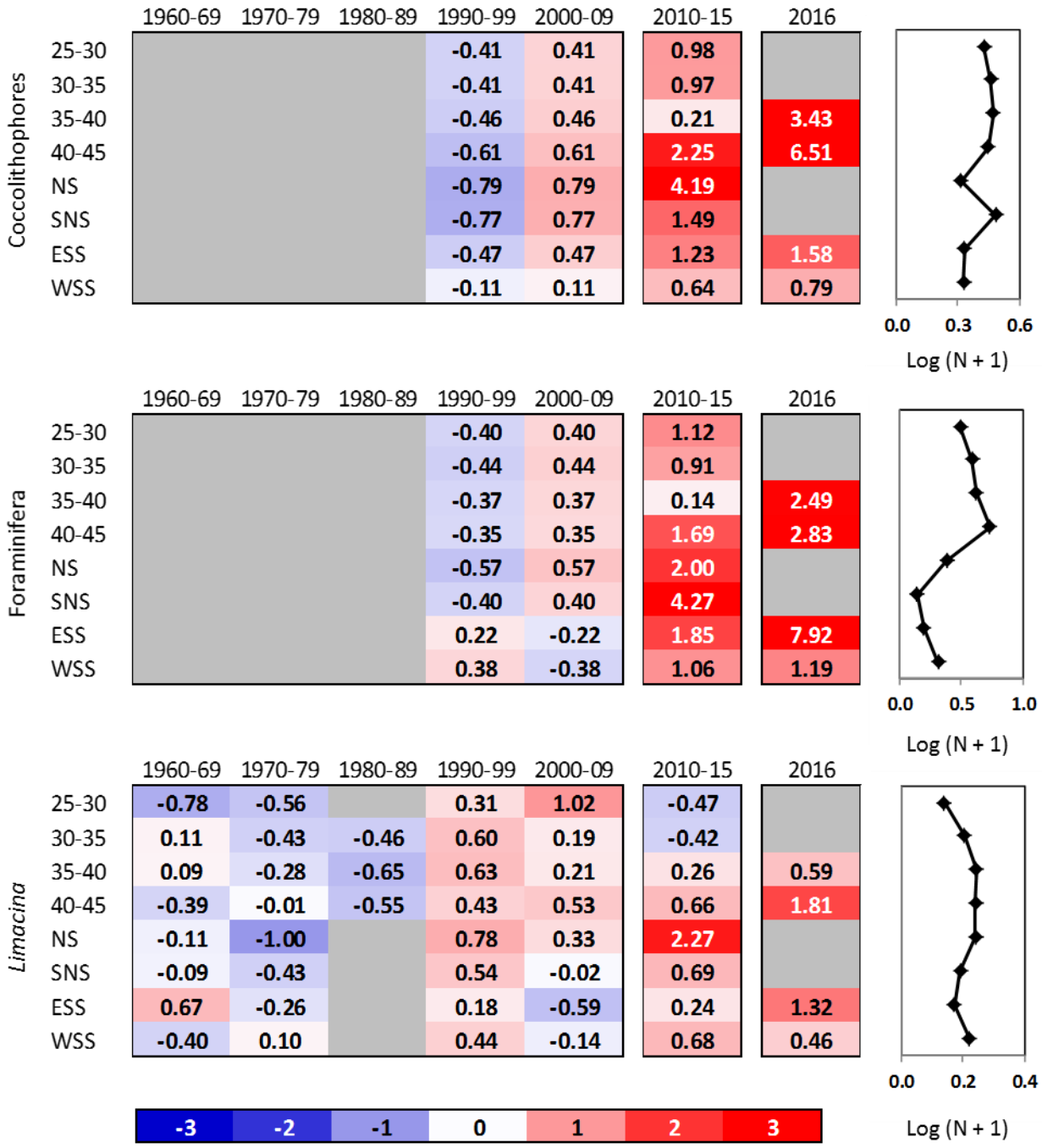

Figure 20. Scorecards for long-term (1960-2016) CPR time series for three acid-sensitive plankton taxa in eight regions in the NW Atlantic. Details as for Figure 16.

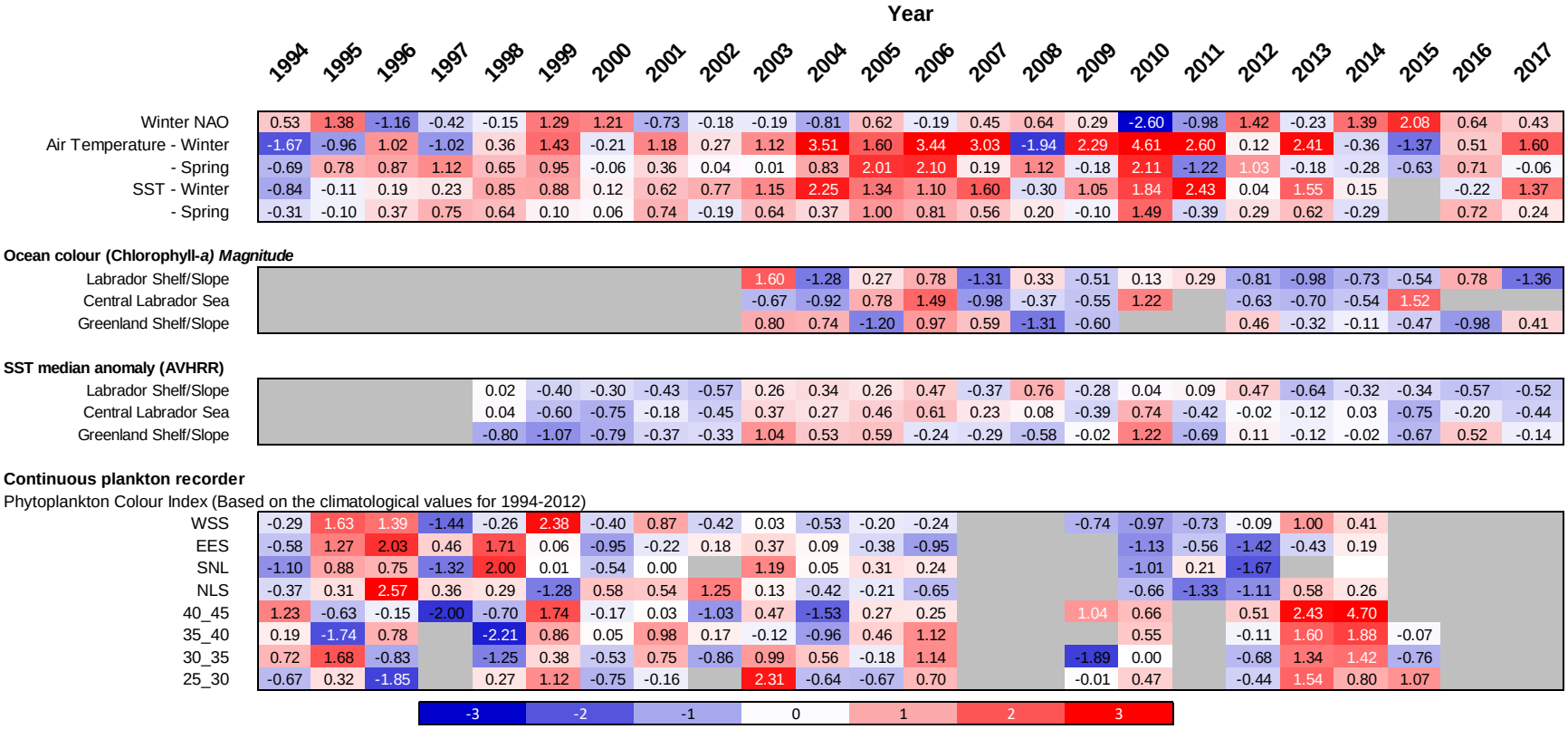

Figure 21. Normalised annual and/or seasonal anomaly of physical and biological variables integrated over large spatial scales estimated using NCEP, remote sensed data or Continuous plankton recorder (CPR) between 1994 and 2017.